Advanced Industrial and Engineering Polymer Research xxx (xxxx) xxx

Contents lists available at ScienceDirect

Advanced Industrial and Engineering Polymer Research

journal homepage: http://www.keaipublishing.com/aiepr

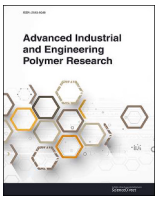

Research paper

# Unexplored Green Solvent Systems for The Preparation of electrospun PLA and PCL functional Membranes: Overcoming Technological Lock-In

Emmanuel Fortunato Gulino, Roberto Scaffaro *

*Department of Engineering, University of Palermo, Viale Delle Scienze Ed. 6, 90128, Palermo, Italy*

A R T I C L E I N F O

*Article history:*
Received 17 November 2025
Received in revised form
28 January 2026
Accepted 10 February 2026

A B S T R A C T

Electrospinning enables the fabrication of nanofibrous membranes with high surface area, tunable porosity, and good mechanical performance. Nevertheless, the vast majority of studies still rely on potentially carcinogenic solvents, such as chloroform (CHF) and dichloromethane (DCM), particularly for polymers like polylactic acid (PLA) and polycaprolactone (PCL). This use reflects a technological lock-in, where hazardous protocols persist despite well documented risks for human health and environment. In this study, acetone, ethanol, and water were investigated as green or green-acceptable alternatives to commonly used solvents for producing electrospun functional membranes. Thermodynamic compatibility was first assessed using Hansen Solubility Parameters (HSP), and their experimentally validated by evaluating solution stability and processability under standard electrospinning conditions. Rheological and morphological analyses confirmed that green solvent-based solutions with adequate proportions allowed producing fibers are comparable to the membrane prepared using hazardous solvent, with additional tunability in terms of fiber diameter and overall morphology. Mechanical testing and wettability measurements further showed properties that are fully comparable to the reference systems, while functional oil absorption tests demonstrated capacities up to 25 g/g with confirmed reusability over five cycles. Finally, the study provides evidence that the long-standing solvent lock-in in electrospinning can be realistically overcome. Crucially, this was achieved without altering the standard process parameters and while obtaining membranes with comparable performances, or in some cases superior, to those fabricated with hazardous solvents.


## 1. Introduction

Electrospinning has emerged as one of the most versatile techniques for the fabrication of fibrous membranes, owing to its ability to produce structures with unique properties such as high surface area, high porosity, good flexibility, high loading capacity, and, above all, good biocompatibility and selectivity [1,2,3,4]. These features make electrospun membranes highly attractive for a wide range of applications, including regenerative medicine, drug delivery, desalination, textiles, smart packaging for food preservation, and, most importantly, the removal of pollutants from air and water [5,6,7,8,9,10,11,12,13,14,15,16].

Despite its wide diffusion, electrospinning still faces a critical issue in terms of environmental and human health safety. In fact, the majority of protocols reported in the scientific literature and applied to an industrial level still rely on highly toxic or potentially carcinogenic solvents. Among these, chloroform and dichloromethane are the most widely used, particularly for the processing of polymers such as polylactic acid (PLA) and polycaprolactone (PCL), both extensively employed in diverse application fields [8,9,17,18,19,20,21]. The harmful effects of these solvents on liver, lungs, and central nervous system have been known since 1980, but only in the early 2000s, thanks to increasing scientific evidence, they were officially listed as substances subject to regulatory restrictions [22,23,24,25]. Nevertheless, their use remains widespread, likely due to the large body of comparable data

* Corresponding Author
*E-mail address:* Roberto.Scaffaro@unipa.it (R. Scaffaro).
Peer review under the responsibility of editorial board of Chinese Journal of Mechanical Engineering.

https://doi.org/10.1016/j.aiepr.2026.02.001


Please cite this article as: E.F. Gulino and R. Scaffaro, Unexplored Green Solvent Systems for The Preparation of electrospun PLA and PCL functional Membranes: Overcoming Technological Lock-In, Advanced Industrial and Engineering Polymer Research, https://doi.org/10.1016/j.aiepr.2026.02.001

available in the scientific literature and the consolidated validation of existing protocols. This represents a clear example of technological lock-in, that is a strong tendency to retain established solutions not because they are the only viable ones, but because they are perceived as safer in terms of reproducibility, comparability, and expected performance. Moreover, the potential risk associated with the use of hazardous solvents does not arise only during the manufacturing process, but may also persist after processing, as traces of residual solvent can remain embedded within the final material. This aspect is particularly relevant for electrospun membranes, where the high surface area and limited diffusion of solvent vapors can hinder complete solvent removal. Several studies have indeed reported that small amounts of residual solvent may remain trapped within nanofibers even after electrospinning [26, 27, 28, 29, 30].

In recent years, however, there has been a growing interest in identifying more sustainable alternatives. The goal in this direction is to select solvent systems that are not classified as potentially carcinogenic, are less toxic to the environment, and are safer for both operators and end users, in full compliance with health safety regulations [25, 31]. To overcome realistically such a technological lock-in, two main conditions must be met: (i) maintaining the consolidated process procedures to ensure comparability with existing protocols; and (ii) obtaining membranes with comparable performance to the traditional ones, while also allowing for property tuning or improvement depending on the application requirements.

Applied to electrospinning, this means ensuring that polymer solutions meet some fundamental requirements: thermodynamic stability for the entire duration of the process, adequate viscosity to allow solution elongation without capillary breakup, sufficient conductivity to promote jet stretching, and suitable volatility solvent for correct fiber solidification and formation of defect-free surfaces [32, 33, 34]. Only if all these conditions are contextually met it is possible to replace hazardous solvents whit safer ones without sacrificing quality and efficiency, thereby laying the foundation for overcoming the above mentioned lock-in.

In recent years, the use of green solvents in electrospinning has emerged as a well-defined and rapidly growing research field, driven by the need for safer and more sustainable processing routes [35, 36].

Green solvent electrospinning has also enabled emerging applications in areas such as personal thermal management, biomedical devices, and separation technologies, where safety and sustainability are critical requirements [37, 38, 39].

Several studies have demonstrated the feasibility of replacing hazardous solvents with greener alternatives, highlighting both the potential of this approach and the remaining challenges related to process robustness, structure-property control, and reproducibility [35,40–42].

In light of these considerations, the aim of this work was to investigate the chance to replace the traditional high toxicity solvents systems with alternative, sustainable, and safer ones, allowing the effective electrospinning of nanofibrous membranes of PLA and PCL.

PLA and PCL were selected as model polymers due to their biodegradability, processability, and widespread use in environmental and biomedical applications. PLA is a partially biobased, biodegradable polyester derived from renewable resources, offering good mechanical properties and strong industrial relevance, while PCL is a biodegradable aliphatic polyester characterized by high flexibility, low glass transition temperature, and excellent compatibility with electrospinning processes. These features make PLA and PCL representative platforms for assessing the feasibility of green solvent electrospinning in applications requiring both sustainability and functional performance [19, 43, 44, 45, 46, 47]

The choice of solvents was based on sustainability criteria already recognized in the literature, namely: EHS (Environment, Health, and Safety), LCA (Life Cycle Assessment), and CED (Cumulative Energy Demand) [25, 48, 49]. According to these parameters, water and ethanol are classified as green solvents, while acetone is considered a green acceptable alternative [25], representing in any case a definitely safer and more sustainable alternative compared to chloroform and dichloromethane.

Beyond demonstrating solvent substitution, this study aims to provide a systematic and process-oriented framework in which green solvent systems are implemented without modifying conventional electrospinning parameters, thus ensuring direct comparability with conventional protocols. In this context, morphological, mechanical, and functional properties of the resulting membranes were evaluated to verify whether performance comparable, or in some cases superior, to that obtained with hazardous solvents can be achieved. Functional performance was specifically assessed through oil spill clean-up tests. Ultimately, this work seeks to provide a concrete and reproducible basis for overcoming the long-standing techno-scientific lock-in that still links electrospinning to the use of hazardous solvents.

## 2. Materials and method

### 2.1. Materials

Polylactic acid (PLA, NatureWorks, 2003D grade; molecular weight 120,000 g/mol) was purchased from NatureWorks. Polycaprolactone (PCL, average molecular weight 80,000 g/mol) was obtained from Sigma-Aldrich. The solvents employed in this study included acetone (Ac), ethanol (Et), and distilled water ($H_2O$) as green alternatives, instead, chloroform (CHF) and dichloromethane (DCM) as conventional high toxicity references were supplied by Sigma-Aldrich.

### 2.2. Solubility evaluation using Hansen solubility parameters (HSP)

A preliminary thermodynamic analysis was performed to evaluate the compatibility between the selected polymers (PLA and PCL) and the investigated solvent systems (acetone, acetone/ethanol, and acetone/water) by means of Hansen Solubility Parameters (HSP). The three HSP components considered were: $\delta_d$ (dispersion forces), $\delta_p$ (polar interactions), and $\delta_H$ (hydrogen bonding). The HSP values for PLA, PCL, and the solvents were obtained from literature [50, 51, 52]. For all the binary solvent mixtures, the overall HSP values were calculated as the volume-fraction weighted average of the individual components.

The solubility distance ($R_a$) between a polymer and a solvent system was calculated according to the following Eq.1:

$$Ra = \sqrt{4\left(\delta_d^P - \delta_d^S\right)^2 + \left(\delta_P^P - \delta_p^S\right)^2 + \left(\delta_h^P - \delta_h^S\right)^2} \quad (1)$$

Where superscripts $_P$ refers to polymer while $_S$ superscripts refer to solvent systems. Each polymer was associated with a solubility sphere defined by a characteristic radius $R_0$. Compatibility between the polymer and the solvent mixture was evaluated based on the ratio $Ra/R_0$, in particular:

$R_a/R_0 < 1$: the solvent is considered theoretically compatible

$R_a/R_0 > 1$: the solvent is considered not compatible.

### 2.3. Preparation of polymeric solutions

Green polymeric solutions were prepared at a polymeric concentration of 10 % w/w by dissolving the selected polymer in

different solvent systems under magnetic stirring. PLA solutions were dissolved at 70 °C overnight to ensure complete solubilization, while PCL solutions were dissolved at 50 °C under the same conditions.

The solvent systems investigated included pure acetone, acetone/ethanol mixtures, and acetone/water mixtures at different ratios. The complete list of compositions and the corresponding sample codes are reported in Table 1.

Polymeric solutions with commonly used high toxicity solvents were prepared at a 10 % w/w concentration and dissolved at 25 °C for 8 hours under continuous magnetic stirring to ensure complete solubilization.

Two distinct systems were prepared based on PLA and PCL, using binary solvent systems. In particular CHF/Ac 66/33 for PLA and DCM/Et 80/20 for PCL, denominated PLA/CHF e PCL/DCM respectively.

### 2.4. Preparation of fibers membranes

All the polymeric solution systems selected were electrospun using a Linari Engineering electrospinning setup. The process parameters were kept constant for all samples. In detail, distance needle to collector 15 cm, voltage applied 15 kV, flow rate 3 mL/h, temperature 25 °C, electrospinning time 4 hours. All the solution were electrospun on a cylindrical dynamic collector.

### 2.5. Rheological analysis

Rheological measurements were performed using an ARES G2 rheometer (TA Instruments) equipped with a 25 mm parallel plate geometry (stainless steel, 0.8 mm) at a controlled temperature of 25 °C. Each solution was subjected to frequency sweeps from 0.1 to 100 rad/s.

### 2.6. Intrinsic viscosity and Berry number calculation

To assess the molar mass of PLA and PCL, intrinsic viscosity measurements were carried out. The polymers were dissolved in chloroform. The polymer solutions were directly diluted with chloroform to obtain dilute solutions with a concentration of 0.13 wt%, according to previous works [53].

Flow time measurements were performed using an iVisc LMV 830 Lauda Proline PV 15 viscometer (Lauda-Königshofen, Germany) equipped with an Ubbelohde capillary viscometer (K = 0.009676), placed in a thermostated oil bath at 30 °C. The intrinsic viscosity [η] was calculated using the Solomon–Ciuta equation (Eq. 2) [54].

$$[\eta] = \frac{\sqrt{2}\,(\eta_s - \ln \eta_r)}{C} \tag{2}$$

The viscometric molar mass (Mv) of PLA and PCL was then calculated using the Mark–Houwink–Sakurada relationship (Eq. 3):

$$M_v = \left(\frac{[\eta]}{K}\right)^{1/\alpha} \tag{3}$$

The Mark–Houwink constants used were K = 0.0153 mL $g^{-1}$ and α = 0.759 for the PLA/chloroform system at 30 °C, and K = 1.298 × $10^{-2}$ mL $g^{-1}$ and α = 0.828 for the PCL/chloroform system at 30 °C.

To evaluate the degree of chain overlap and entanglement in the polymer solutions, the Berry number (Be) was calculated as a dimensionless processing parameter commonly adopted in electrospinning studies.

The Berry number is defined as Eq. 4:

$$B_e = [\eta]^* C \tag{4}$$

where $[\eta]$ is the intrinsic viscosity of the polymer, in dL/g, and $C$ is the polymer concentration, in g/dL.

According to literature, $B_e$ provides an effective criterion to distinguish between dilute, semi-dilute unentangled, and semi-dilute entangled regimes, with $B_e \approx 1$ corresponding to the onset of chain overlap and $B_e > 1$ indicating conditions suitable for continuous fiber formation during electrospinning [55, 56].

In this work, intrinsic viscosity values were experimentally determined for both PLA and PCL, and Berry numbers were calculated for all solvent systems to verify that the solutions fall within the entangled regime required for stable electrospinning.

### 2.7. Electrical conductivity of the solutions

The electrical conductivity of the polymeric solutions was measured at room temperature (25 °C) using a conductivity meter (Xylem, Weilheim in Oberbayern, Germany) equipped with a standard conductivity cell (cell constant K = 1.0 $cm^{-1}$). Measurements were performed on 20 mL of solution, immediately after preparation, and repeated three times for each sample. The average values, expressed in μS/cm, are reported together with the corresponding standard deviations.

### 2.8. Morphological characterization

Morophological characterization of electrospun membranes was carried out using a scanning electron microscopy (SEM) Phenom ProX (Phenom-World, The Netherlands) with acceleration voltages of 15 kV. The microscope is equipped with a temperature controlled (25 °C) sample holder. The samples were positioned on an aluminium stub using an adhesive carbon tape and sputtered with a thin of layer gold to enhance surface electrical conductivity. SEM images were processed using ImageJ software. In order to evaluate fiber diameter distribution for each sample, the diameter of over 100 fibers were measured. The results were reported as mean ± standard deviation, and fiber diameter distributions were shown using frequency histograms to evaluate the influence of solvent composition on fiber morphology.

### 2.9. Mechanical characterization

Mechanical performance of the electrospun membranes was evaluated through tensile tests carried out using a universal testing machine (Instron model 3365, UK) equipped with a 1 kN load cell

**Table 1**
sample code and their relative compositions

| Polymer | Solvent system | Ratio (v/v) | Sample code |
|---|---|---|---|
| PLA | Acetone | 100/0 | PLA /Ac100 |
| PLA | Acetone/Ethanol | 80/20 | PLA/AcEt8020 |
| PLA | Acetone/Ethanol | 90/10 | PLA/AcEt9010 |
| PLA | Acetone/Ethanol | 95/5 | PLA/AcEt9505 |
| PLA | Acetone/Water | 90/10 | PLA/AcW9010 |
| PLA | Acetone/Water | 95/5 | PLA/AcW9505 |
| PLA | Acetone/Water | 80/20 | PLA/AcW8020 |
| ***PLA*** | ***Chloroform/acetone*** | ***66/33*** | ***PLA/CHF*** |
| PCL | Acetone | 100/0 | PCL/Ac100 |
| PCL | Acetone/Ethanol | 80/20 | PCL/AcEt8020 |
| PCL | Acetone/Ethanol | 90/10 | PCL/AcEt9010 |
| PCL | Acetone/Ethanol | 95/5 | PCL/AcEt9505 |
| PCL | Acetone/Water | 90/10 | PCL/AcW9010 |
| PCL | Acetone/Water | 95/5 | PCL/AcW9505 |
| PCL | Acetone/Water | 80/20 | PCL/AcW8020 |
| ***PCL*** | ***Dichloromethane/Ethanol*** | ***80/20*** | ***PCL/DCM*** |

and with the BioPulse system, specifically designed for the gripping of electrospun mats. Rectangular specimens (10 × 90 mm) were cut from the membranes, and tests were performed using a dual crosshead speed: 1 mm $min^{-1}$ for the first 2 minutes and 50 mm $min^{-1}$ until sample failure. The grip distance was set to 20 mm, and the sample thickness was measured before each test. All measurements were conducted in triplicate, and the obtained values of elastic modulus (E), tensile strength (TS), and elongation at break (EB) are reported as mean values ± standard deviations

### 2.10. Thermogravimetric analysis

Thermogravimetric analysis (TGA) was carried out on electrospun PLA- PCL based nanofibrous membranes to evaluate their thermal stability at low temperatures. The measurements were performed using a Netzsch STA 449 F1 thermobalance operating in dynamic mode under a nitrogen atmosphere.

Approximately 3 mg of each membrane sample was placed in an alumina crucible and heated from 30 °C to 120 °C at a constant heating rate of 10 °C/min. The selected temperature range was specifically chosen to detect possible mass losses associated with residual solvent or water trapped within the nanofibrous structure, without inducing polymer thermal degradation.

All measurements were carried out under identical experimental conditions to allow a direct comparison among membranes produced using conventional and green solvent systems.

### 2.11. Differential scanning calorimetry

Differential scanning calorimetry (DSC) was performed using a Shimadzu DSC-60 instrument. All measurements were carried out under a nitrogen atmosphere at a constant heating rate of 10 °C $min^{-1}$, within a temperature range of 25-200 °C for PLA and 25-100 °C for PCL.

The degree of crystallinity ($\chi$) of the electrospun membranes was calculated according to Eq. 5:

$$\chi = \frac{\Delta H_m - \Delta H_{\{cc\}}}{(1-\phi_w)\Delta H_m^0} \tag{5}$$

where $\Delta H_m$ is the melting enthalpy, ΔHcc is the cold crystallization enthalpy (when present), Φw is the polymer weight fraction in the sample (equal to 1 for neat polymer membranes), and $\Delta H_m^0$ is the melting enthalpy of a fully crystalline polymer. For PLA, a value of 93.7 J $g^{-1}$ was used, while for PCL a value of 139.5 J $g^{-1}$ was assumed, in accordance with literature data.

### 2.12. Water and oil contact angle

The surface wettability of the electrospun membranes was evaluated by measuring the static water contact angle (WCA) and oil contact angle (OCA) using a First Ten Angstroms FTA 1000 system (UK). A drop of 4 μL distilled water or oil was automatically dispensed onto the membrane surface using a dosing system, and images were captured 1 seconds after deposition.

Measurements were performed on five different spots of each sample, and results were expressed as mean ± standard deviation.

### 2.13. Oil adsorption functional test

The oil absorption capacity of the electrospun membranes was evaluated using two different oils as model pollutants: olive oil (food-grade) and used engine oil (collected after standard automotive use). For each test, 1 g of membrane sample was accurately weighed ($W_0$) and placed in a beaker containing both water and olive oil or exhaust motor oil, which were present as separate phases. After removal, the samples were gently drained on filter paper to remove surface excess and immediately weighed again (Wf).

The oil absorption capacity (Q, g oil/g membrane) was calculated according to the following Eq. 6:

$$Q = \frac{W_f - W_0}{W_0} \tag{6}$$

where *Wf* is the final weight of the membrane after oil uptake and $W_0$ is the initial dry weight.

All the experiments were carried out in triplicate and average values with standard deviations are reported.

To investigate the absorption kinetics, time-dependent oil uptake experiments were performed using exhaust motor oil, as it better represents realistic oil spill conditions. During these tests, membrane samples were immersed in the oil systems and removed at predefined time intervals. After a brief draining step to remove excess oil, the membrane weight was recorded.

The oil absorption capacity as a function of time $Q_t$ was calculated using Eq. 7:

$$q_t = \frac{W_t - W_0}{W_0} \tag{7}$$

where $W_t$ is the weight of the membrane at a given absorption time *t*, and $W_0$ is the initial dry weight of the membrane.

All absorption experiments were performed at room temperature, and each test was repeated at least three times to ensure reproducibility.

To quantitatively assess the preferential affinity of the electrospun membranes toward oil in the presence of water, oil and water uptake tests were performed independently under controlled conditions in accordance with previously reported methodologies for evaluating oil/water selectivity in fibrous sorbents [57].

For oil selectivity measurements, membrane samples were first tested in pure oil systems to determine the oil absorption capacity (Q_oil), following the procedure described above and calculated according to Eq. (6). In parallel, water uptake experiments were conducted by immersing dry membrane samples (initial weight $W_0$) in deionized water for a fixed time. After removal, the samples were gently drained on filter paper to eliminate surface excess and immediately weighed.

The water absorption capacity ($Q_{water}$, $g_{water}/g_{membrane}$) was calculated using Eq. 8:

$$Q_{water} = \frac{W_w - W_0}{W_0} \tag{8}$$

where $W_w$ is the membrane weight after water uptake and $W_0$ is the initial dry weight.

Based on the independently measured oil and water absorption capacities, the oil-to-water selectivity index $S_{O/W}$ was calculated according to Eq. 9:

$$S_{o/w} = \frac{Q_{oil}}{Q_{water}} \tag{9}$$

where $Q_{oil}$ is the oil absorption capacity ($g_{oil}/g_{membrane}$) calculated from Eq. 2, and $Q_{water}$ is the water absorption capacity ($g_{water}/g_{membrane}$) obtained from Eq. 8.

The oil-to-water selectivity index provides a quantitative measure of the membrane's preferential oil absorption over water.

All oil and water uptake experiments were carried out at room temperature, repeated at least three times, and average values with standard deviations are reported.

### 2.14. Morphological stability and reusability

Structural stability and reusability of the electrospun membranes were evaluated through cyclic oil absorption and regeneration tests. Membrane samples (1g) were subjected to repeated oil spill clean-up and washing tests using used engine oil as the model pollutant. After each absorption step, the membranes were cleaned with a standardized washing procedure (water and mild detergent), dried at room temperature, and reused for the subsequent cycle. The absorption capacity was measured up to five cycles following the method described above.

To assess morphological stability, the membranes were analyzed by scanning electron microscopy (SEM) after the first oil spill clean-up and after the fifth reuse cycle. This allowed correlating possible structural changes in the fibrous network with the evolution of the absorption capacity over repeated use.

## 3. Results and discussion

To assess the potential presence of residual solvents, FTIR analysis was performed on membranes produced using hazardous solvent systems, namely PLA/CHF and PCL/DCM.

Figure 1 shows the FTIR spectra, with absorbance plotted as a function of wavenumber for PLA/CHF (Figure 1a) and PCL/DCM (Figure 1b), before and after thermal treatment in an oven overnight (70 °C for PLA and 30 °C for PCL). In the same figure, inset magnifications of the spectral regions between 1000 and 500 $cm^{-1}$ for PLA and 1070 and 1020 for PCL are also reported in order to detect the characteristic peaks of chloroform (750 $cm^{-1}$, C–Cl vibrations with contributions from C–H bending) and dichloromethane (1045 $cm^{-1}$, out-of-plane C–Cl deformations) before and after thermal treatment,

Apart from the typical and recognizable bands characterizing PLA and PCL [18, 58] as highlighted in the inset magnifications, the characteristic bands attributable to chloroform at 750 $cm^{-1}$ (inset Fig. 1a related to PLA membranes) and dichloromethane at 1045 $cm^{-1}$ (inset Fig 1b related to PCL membrane) are clearly identificable. In both cases, a reduction in band intensity is observed after oven thermal treatment, suggesting a partial solvent evaporation during this process. However, the persistence of these peaks (even after 12 hours in the oven) clearly indicates the presence of residual solvents trapped within the fibers in all the cases. More in detail, during electrospinning, small solvent traces may remain physically trapped within the nanofibrous structure or in polymer matrix or, more likely, as temporary residuals on the membrane surface, particularly at the fiber junctions, even for highly volatile solvents. These residuals are likely those that are detected by FTIR-ATR analysis: they are not significantly affecting the overall performance of the materials (see also below) but are however detected by the instruments.

This phenomenon, already reported in the scientific literature [26, 28, 29, 30], represents a potential limitation in the use of the membranes, where safety and material purity are critical requirements such as biomedicine and environmental applications. In addition, safety issues during the preparation and manipulation of the membranes further stimulate to find alternative and more benign solvent systems to achieve the same performance.

In order to evaluate the compatibility between greener solvent systems and the polymers object at the present study, a preliminary analysis of the polymeric solutions was carried out using the Hansen Solubility Parameters (HSP) model. In particular, the ability of green solvents systems to solubilize PLA and PCL was assessed according to Equation 1 and the result are showed in table 2.

Specifically, the table reports the $R_0$ values, corresponding to the solubility radius of each polymer, and the $R_a$ values, which represent the HSP distance between the solvent system and the polymer. According to the HSP theory, a solvent system is considered thermodynamically compatible with the polymer when $R_a \leq R_0$. The table also includes the resulting $R_a/R_o$ value with the consequent solvent polymer compatibility evaluation and the hazardous systems (DCM and CHF) are also included for comparison.

As shown in Table 2, the HSP analysis indicates good thermodynamic compatibility between both polymers and the tested green solvent systems, with $R_a/R_0$ values below unity in most cases. However, when the water content reaches higher levels, the calculated $R_a$ values approach or slightly exceed the solubility radius of the polymer, suggesting a loss of compatibility. Conversely, solvent mixtures containing moderate amounts of water or ethanol remain within the solubility sphere, confirming their potential suitability.

Thermodynamic compatibility is of course necessary but alone is not sufficient to guarantee the processability of solutions by electrospinning. In fact, phenomena, such as chain resolvation, aggregation, or the formation of unstable phases over time, may compromise the processability of the solutions [59, 60]. For these reasons, an additional experimental step analyzing the stability of the solutions oven time was performed. Figure 2 shows the visual appearance of the solutions used to qualitatively assess their solubility and stability after removal from the hot plate and during storage at 25 °C for up to 4 hours, which corresponds to the typical duration of an electrospinning processing session. For PCL-based systems, the starting temperature after heating was approximately 50 °C, while for PLA-based systems it was about 70 °C, after which all solutions were kept at 25 °C throughout the monitoring period. In particular, based on their visual appearance, the solutions were classified into five categories: clear, transparent solution without suspended particles Fig. 2a; slightly turbid, solution with mild opacity Fig.2b; turbid, opaque solution with evident scattering Fig.2c; partially soluble, formation of precipitate or partial phase separation Fig.2d; insoluble, significant or total loss of solubility Fig.2e according to the appearance of the solution shown in figure 2.

In Table 3, the results of the solubility and stability analysis conducted on all the prepared solutions are reported. In detail, the evaluation was carried out at time intervals of 30, 60, 120, and over 300 minutes (approximately 4 h) at room temperature. This assessment is particularly relevant in the context of overcoming the technological lock-in associated with the use of conventional high toxicity solvents, since, although variations in solution appearance may occur over time, it is essential to determine whether such changes actually affect solution processability, as well as the resulting fiber morphology and final membrane properties.

Based on these observations, only the solvent systems that remained soluble or partially soluble throughout the entire monitoring time were selected for further rheological, morphological and functional characterization. Among these, we focused on the formulations containing the highest possible amount of green solvents (ethanol or water), while all compositions exhibiting an insoluble or phase-separated appearance were discarded.

Thermodynamic stability and solvent polymer compatibility alone are not sufficient to guarantee electrospinnability, in fact, it is also necessary to verify whether the selected solutions exhibit suitable rheological behaviour. Rheological behaviour is a key property to evaluate the processability of polymeric solutions, as

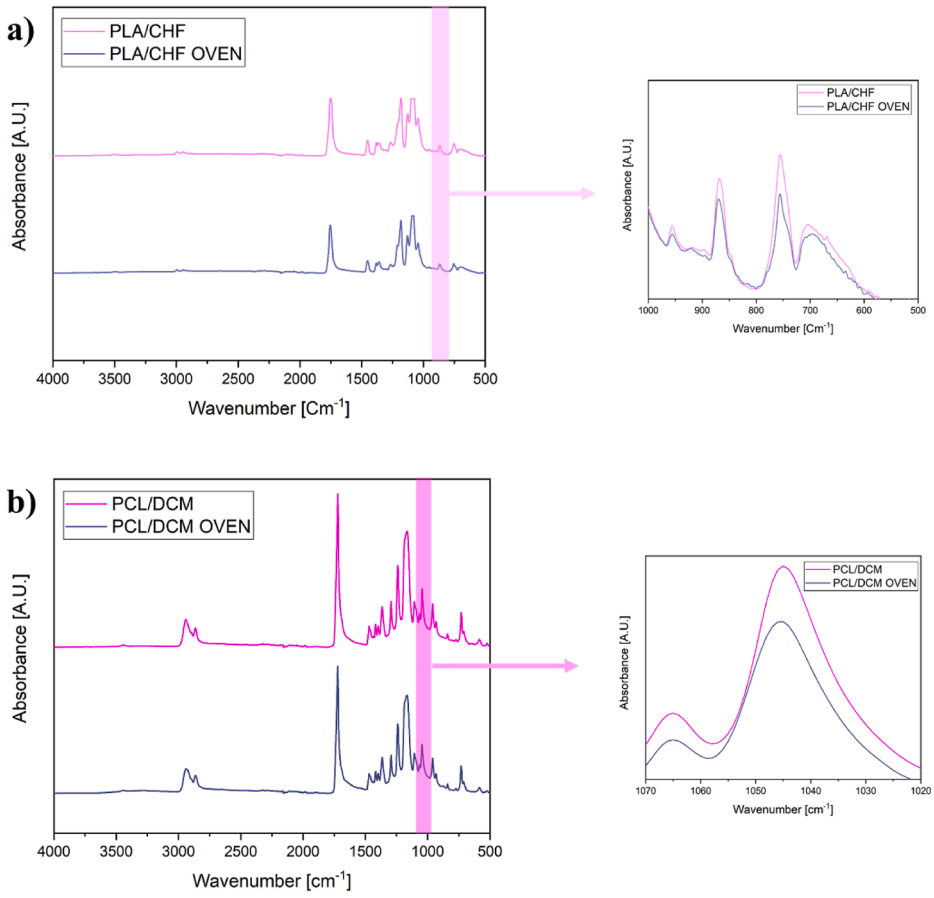


**Figure 1.** bands identification of Chloroform and Dichloromethane for PLA and PCL membranes respectively

**Tab 2**
Hansen solubility parameter (HSP) analysis: $R_0$, $R_a$ and predicted compatibility of each solvent system with PLA and PCL.

| | $R_0$ (Radius solubility of Polymer) | $R_a$ (HSP systems distance) | $R_a/R_0$ | Solvent system compatibility |
|---|---|---|---|---|
| PLA/CHF | 10 | 8.1 | 0.81 | Yes |
| PLA /Ac100 | | 6.3 | 0.63 | Yes |
| PLA/AcEt8020 | | 7 | 0.7 | Yes |
| PLA/AcEt9010 | | 6.5 | 0.65 | Yes |
| PLA/AcEt9505 | | 6.3 | 0.63 | Yes |
| PLA/AcW9010 | | 7.7 | 0.77 | Yes |
| PLA/AcW9505 | | 6.8 | 0.68 | Yes |
| PLA/AcW8020 | | 10.2 | 1.02 | No |
| PCL/DCM | 9.5 | 1.8 | 0.19 | Yes |
| PCL/Ac100 | | 7.1 | 0.75 | Yes |
| PCL/AcEt8020 | | 6.7 | 0.71 | Yes |
| PCL/AcEt9010 | | 6.8 | 0.72 | Yes |
| PCL/AcEt9505 | | 6.9 | 0.73 | Yes |
| PCL/AcW9010 | | 7.7 | 0.81 | Yes |
| PCL/AcW9505 | | 7.1 | 0.75 | Yes |
| PCL/AcW8020 | | 9.7 | 1.02 | No |

shear viscosity strongly influences jet formation and stability For this reason, a rheological analysis was conducted using a parallel plate rheometer.

In Figure 3, the complex viscosity (η*) values as a function of angular frequency are shown for PLA and PCL based solutions. Figure 3a displays the systems prepared with PLA, which exhibit an almost uniform behavior among all the solvent systems analyzed. In all the cases, the complex viscosity decreases with increasing frequency, maintaining a comparable trend between the green solutions and the conventional reference system based on chloroform (PLA CHF). Only small differences can be observed in the low frequency region, in particular, PLA/AcW9505 and PLA/AcEt9010 solutions show slightly higher viscosity values compared to the reference systems [9, 46, 61], while PLA/100Ac, exhibits an intermediate behavior, with viscosity values between those of the other systems and CHF. Overall, the rheological behavior of PLA, suggests that the use of alternative solvents does not compromise the processability of the polymer.

A different trend is observed for the PCL solutions (figure 3b). PCL/DCM shows a typical behavior, characterized by the presence

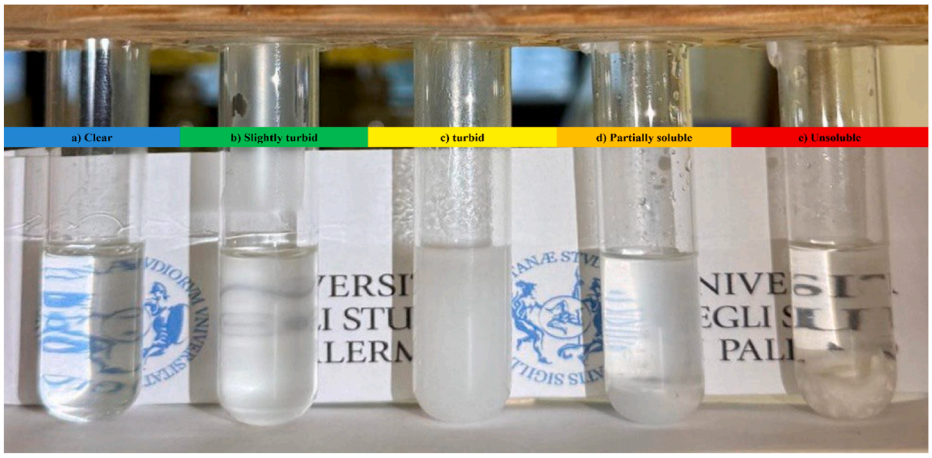


**Figure 2.** Visual criteria adopted to classify the solubility and stability of the solutions. Images a)–e) are representative examples selected to illustrate the appearance of solutions at different stages. Specifically: a) PCL/AcEt9010, b) PCL/AcW9010, c) PLA/Et9010 observed after 120 min at 25 °C; d) PLA/AcW9010 and e) PLA/Et8020 after 300 min at 25 °C.

**Table 3**
Solubility behaviour of PLA and PCL solutions monitored during cooling to 25 °C and after 30, 60, 120 and 300 min

| | Solubility after 30 min at 25 °C | Solubility after 60 min at 25 °C | Solubility after 120 min at 25 °C | Solubility after 300 min at 25 °C |
|---|---|---|---|---|
| PLA/CHF | Clear | clear | clear | clear |
| PLA/Ac100 | clear | slightly turbid | turbid | turbid |
| PLA/AcEt9505 | clear | slightly turbid | turbid | turbid |
| PLA/AcEt9010 | clear | slightly turbid | turbid | turbid |
| PLA/AcW9505 | clear | slightly turbid | turbid | turbid |
| PLA/AcW9010 | partially soluble | partially soluble | insoluble | insoluble |
| PLA/ACW8020 | partially soluble | partially soluble | insoluble | insoluble |
| PLA/AcEt8020 | partially soluble | partially soluble | insoluble | insoluble |
| PCL/DCM | clear | clear | clear | clear |
| PCL/Ac100 | clear | clear | clear | clear |
| PCL/AcEt9505 | clear | clear | clear | clear |
| PCL/AcEt9010 | clear | clear | clear | clear |
| PCL/AcW9505 | clear | clear | clear | clear |
| PCL/AcW9010 | slightly turbid | turbid | turbid | partially soluble |
| PCL/AcW8020 | partially soluble | partially soluble | insoluble | insoluble |
| PCL/AcEt8020 | clear | clear | clear | clear |

of a well-defined Newtonian region at low frequencies, and a shear-thinning at higher frequencies. A similar trend, although with lower viscosity values and shear thinning beginning at lower frequencies, is observed for the ethanol-based systems, particularly PCL/AcEt8020 and PCL/AcEt9505, among these, the latter shows the lowest viscosity values overall. In contrast, the systems containing water exhibit a markedly different rheological response, in particular, both PCL/AcW9505 and PCL/AcW9010 do not show a Newtonian region while showing an immediate viscosity decrease already even at the lowest tested frequencies.

The differences suggest that, probably, ethanol based systems promote a better solubilization of PCL chains, also accorded to previous thermodynamic compatibility analysis. In particular, ethanol-based systems exhibited a behaviour comparable to the reference system, confirming their good thermodynamic compatibility. Conversely, water-based systems, in which showed an earlier viscosity drop, as expected from their higher $R_a/R_0$ ratios and visual evidence of reduced solubility, indicating that the presence of water likely worsens polymer solubilization compared to ethanol.

On the whole, the rheological analysis confirms that, despite some slight variations especially in the PCL-based systems, the tested green solvents ensure complex viscosity values compatible with a stable electrospinning process [8, 9, 61], without penalizing processability compared to hazardous systems.

Another critical characteristic affecting the electrospinning process is the electrical conductivity of the solutions. Indeed, during electrospinning, the stretching and stability of the polymer jet are strongly affected by the electrical charge density within the solution, which conversely depends on its conductivity. In this sense, to verify the compatibility of the solutions with ES using the non benign solvent systems, electrical conductivity measurements were performed on all the systems, and the results are presented in Table 4.

In detail, all PLA based solutions show low conductivity values, ranging from 1.1 to 2.9 μS/cm. The reference system PLA/CHF exhibits the lowest value (1.1 μS/cm). Slightly higher values are recorded for PLA/Ac100 (1.5 μS/cm) and PLA/Et9505 (1.8 μS/cm), while the highest conductivity among PLA systems is observed for PLA/W9505 (2.9 μS/cm).

The PCL-based systems show a wider range of conductivity values. The reference PCL/DCM solution records 1.9 μS/cm, while PCL/Et9505 shows a similar value (1.1 μS/cm) and PCL/AcEt8020 records the value of 1.3 μS/cm. A progressive increase is observed in the systems containing water: PCL/AcW9505 reaches 2.5 μS/cm, PCL/AcW9010 rises to 7.2 μS/cm.

Overall, these results highlight the significant influence of solvent composition on the electrical properties of the solutions. In particular, systems containing water tend to exhibit higher conductivity, while those based on acetone or ethanol show lower

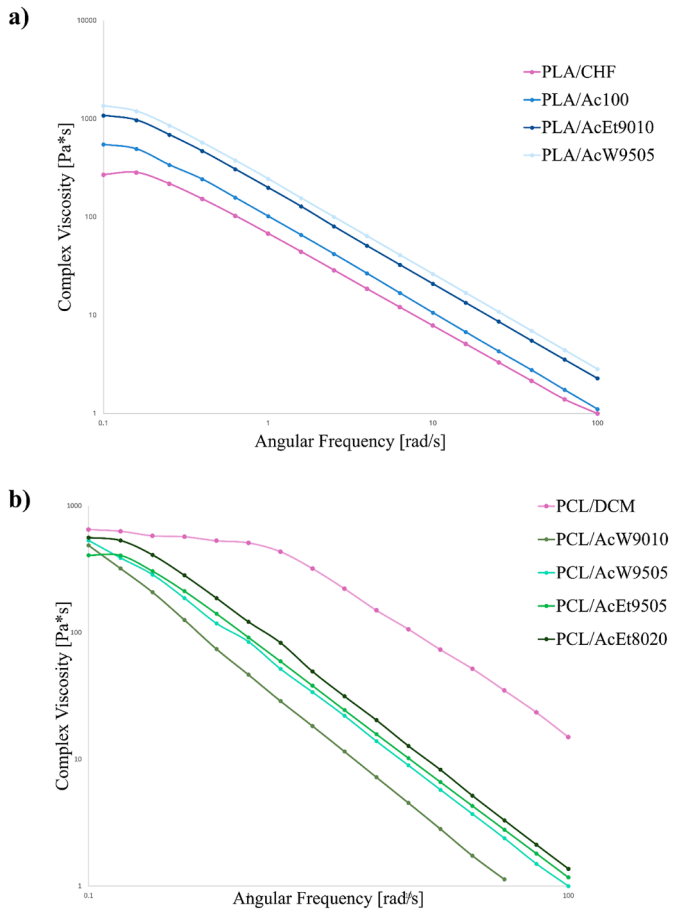


**Figure 3.** Complex viscosity (η*) as a function of angular frequency for (a) PLA- and (b) PCL-based solutions prepared with hazardous and green solvent systems.

**Table 4**
conductivity of polymeric solutions

| Polymeric solution | Conductivity (μS/cm) |
|---|---|
| PLA/CHF | 1.1 |
| PLA/Ac100 | 1.5 |
| PLA/AcEt9505 | 1.8 |
| PLA/AcW9505 | 2.9 |
| PCL/DCM | 1.9 |
| PCL/AcEt9505 | 1.1 |
| PCL/AcEt8020 | 1.3 |
| PCL/AcW9505 | 2.5 |
| PCL/AcW9010 | 7.2 |

values. This trend reflects the increasing polarity and dielectric constant of the solvent mixture, which are expected to affect charge transport and, consequently, the electrospinning process. Moreover, the increase in electrical conductivity promotes a more efficient stretching of the polymer jet during electrospinning contributes to the formation of thinner, defect-free nanofibres improving fiber formation [35]. It should be noted that the measured conductivity refers to polymer solutions rather than to the ethanol/water solvent mixture alone. In particular, the presence of electrically insulating polymers such as PLA and PCL is expected to significantly reduce the overall conductivity of the system [35, 62, 63, 64].

To verify if the combination of all the characteristics translates into good processability, the PLA-based solutions were electrospun and the membranes obtained were morphologically analyzed by SEM Fig.4. In particular, in the case of PLA/CHF Fig.4a, the fibers exhibited an average diameter distribution about 1 μm, characterized by good uniformity and absence of relevant defects. Instead, in the PLA/Ac100 system Fig.4b, the diameter distribution becomes broader and the mode shifted toward higher values, about 1.6 μm, showing a slight increase compared to the hazardous reference system. A comparable behaviour was also found for PLA/AcEt9010 Fig.4c, which displayed similar average diameters and a wide but regular distribution. A different situation was observed for the PLA/AcW9505 system Fig.4d, where the addition of water led to a reduction in the average fiber diameter, with a mode about 0.7 μm, indicating greater jet elongation during electrospinning.

This evidence is according to the conductivity data (table 4), in particular, the introduction of small amounts of water into acetone-based solutions resulted in an increase in electrical conductivity. This promoted higher charge accumulation on Taylor cone and, consequently, more intense electrostatic stretching of the jet, leading to the formation of thinner and more uniform fibers.

As regard PCL-based membranes (Figure 5), the behaviour was more surprising. In particular, PCL/DCM systems Fig.5a, exhibited a fiber-only morphology with a slightly multimodal distribution and average diameters around 2 μm. Differently, a completely different structure was observed for the PCL/AcEt9505 system Fig.5b, which showed a beads-on-string morphology with fiber diameters around 0.4 μm. With higher ethanol content, in the PCL/AcEt8020 system Fig.5c, a homogeneous structure consisting exclusively in fibers with diameters around 1 μm was obtained. For the systems containing water, two opposite behaviour were observed. Specifically, a fibrous structure with a slight presence of beads was found in the PCL/AcW9505 system Fig.5d, with fiber diameters around 0.7 μm. In contrast, increasing the water content in the PCL/AcW9010 system Fig.5e, resulted in the formation of a highly multimodal and heterogeneous fibrous structure, with diameters ranging from 1.7 to 7 μm and the presence of non-fibrous aggregates.

The achievement of there structures, very different each other, can be explained by intersecting the results obtained from rheological and conductivity characterizations of the solutions. In particular, the presence of beads-on-string can be attributed to the strong instability of the solution, with slightly lower viscosity values in the PCL/AcEt9505 system, which also showed lower conductivity compared to the rest of the PCL series. Furthermore, when higher amounts of ethanol were added, as in the case of PCL/AcEt8020, an increase in conductivity was observed (see tab 4), promoting appropriate solution stretching without instability of Taylor's cone, In addition, the higher ethanol content contributes to a more favorable evaporation dynamics due to its high volatility, promoting a more uniform jet solidification and suppressing bead formation, as also reported in recent studies on ethanol-containing electrospinning systems [14].

With the addition of water, in the PCL/AcW9505 system, a more stable jet was achieved, resulting in an almost unimodal fibrous structure nearly free of beads. On the other hand, when a higher amount of water was added in the PCL/AcW9010 system, a strongly multimodal and heterogeneous fibrous structure with aggregates was formed. Despite the increase in conductivity, which should induce a better spinnability, this phenomenon can be likely attributed to the low volatility of water, which prevents proper elongation and solvent removal during the solution stretching during the fly in the efficient subsequent retraction of stretched droplet to globular ones.

As well known, electrospinning, beyond some obvious physical parameters (solution temperature, air temperature, air humidity, potential, collector distance/position/relative speed, flowrate …) is

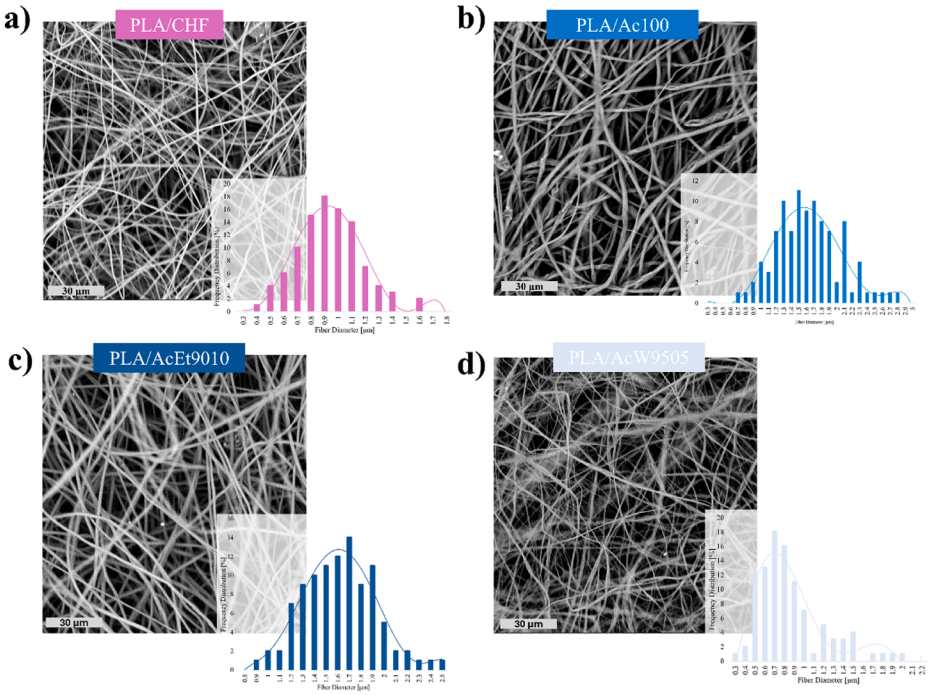


**Figure 4.** Morphological characterization of PLA-based electrospun membranes prepared using hazardous (PLA/CHF) and green solvent systems (PLA/Ac100, PLA/AcEt9010 and PLA/AcW9505). SEM micrographs and corresponding fiber diameter distributions are reported for each formulation.

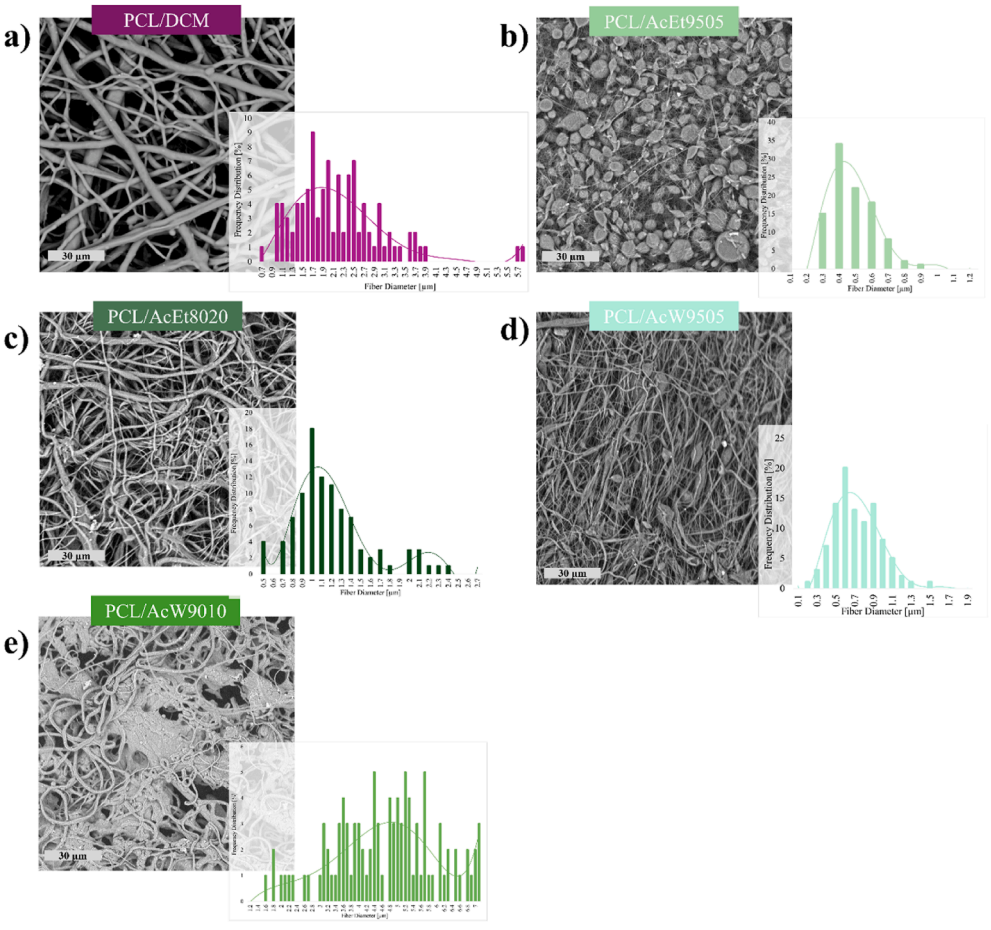


**Figure 5.** SEM images and fiber diameter distributions of PCL membranes electrospun from hazardous (PCL/DCM) and green solvent systems (PCL/AcEt9505, PCL/AcEt8020, PCL/AcW9505 and PCL/AcW9010)

affected by other relevant variables such as: polymer concentration, solution viscosity, elongational properties of the solutions. The effects of this complex set of variables affecting the operation is often difficult to identify as single contributions, even if some experimental approaches can help in analyzing them. In this sense, oscillatory shear rheology and Berry number analysis [65, 66] can help to further assess the viscoelastic response of the solutions and to obtain a semi-quantitative criterion to verify the potential spinnability of the solutions [56, 65, 66]. In detail, Berry number was used by several researchers as a practical processing index to evaluate/control the formation of fibers during processing. The results indicate that all the systems exhibited comparable G′ and G″ profiles and Berry number values higher than unity, confirming that the solutions operate within the chain-entangled regime, despite the occurrence of beads-on-string morphologies (see Figure S1 and Table S1).

To exclude polymer degradation as a contributing factor to the observed morphological differences, intrinsic viscosity measurements were performed on both PLA and PCL systems after the dissolution protocol. The obtained intrinsic viscosity and viscometric molecular weight values show no significant variations among the different solvent systems, indicating that the polymer molecular weight is not appreciably affected (see table S2).

The different solvent systems adopted may influence the mechanical behaviour of the membranes. For this reason to evaluate the effect of the solvent on the final properties of the membranes, the values of elastic modulus (E), tensile strength (TS), and elongation at break (EB), of membranes obtained with green solvents were compared with those of the conventional systems and the results are shown in table 5.

In particular, PLA/CHF sample, exhibited the highest elastic modulus (E ≈ 52 MPa), moderate elongation at break (EB ≈ 36 %), and a TS of about 1.08 MPa. Among the green systems, PLA/Ac100 maintained good tensile stress (TS ≈ 1.6 MPa) and showed an increase in elongation (EB ≈ 46 %), suggesting higher ductility, while the modulus decreased to about 40 MPa. PLA/AcEt 9010 also showed comparable mechanical values, with a slightly lower modulus (E ≈ 43 MPa) and a strength similar to the CHF reference, although elongation was more limited (EB ≈ 17 %). A more evident reduction was observed for the PLA/AcW9505 system, where both E (≈24 MPa) and TS (≈0.4 MPa) were lower, likely consistent with the presence of a fibrous structure with thinner diameters.

The behavior of PCL appeared more heterogeneous. The reference PCL/DCM system showed a relatively low modulus (≈7 MPa) and moderate elongation (≈28 %). Among the green systems, distinct differences related to morphology were observed: PCL/AcEt9505 exhibited the lowest values of modulus and strength (E ≈ 5 MPa; TS ≈ 1 MPa), with a higher EB (≈39 %), consistent with the presence of beads-on-string and a less compact fibrous network. In contrast, PCL/AcEt8020 showed a more balanced performance, with a slight increase in TS (≈1.36 MPa) and E (≈10 MPa), combined with good deformability (EB ≈ 31 %). Water-based systems provided interesting results: PCL/AcW9505 combined a higher modulus (≈16 MPa) with elevated ductility (EB ≈ 45 %), whereas PCL AcW/9010 achieved the maximum elongation (EB ≈ 70 %), in line with a morphology closer to film-like structures rather than fibers, and a tensile strength comparable to the reference systems and in the typical range reported in the scientific literature for similar systems [67, 68, 69, 70, 71].

**Table 5**
Mechanical properties of electrospun PLA- and PCL-based membranes prepared using hazardous and green solvent systems.

| SAMPLE | E (MPa) | TS (MPa) | EB (%) |
|---|---|---|---|
| PLA/CHF | 52.62 ± 2.1 | 1.08 ± 0.2 | 36.07 ± 3 |
| PLA/Ac100 | 39.72 ± 1.9 | 1.6 ± 0.4 | 45.95 ± 4 |
| PLA/AcEt9010 | 42.53 ± 1.7 | 1.12 ± 0.2 | 16.82 ± 2.7 |
| PLA/AcW9505 | 24.15 ± 1.2 | 0.41 ± 0.1 | 14.66 ± 1.2 |
| ***PCL/DCM*** | ***7.06 ± 0.5*** | ***0.62 ± 0.3*** | ***28.22 ± 2*** |
| PCL/AcEt9505 | 5.24 ± 0.4 | 0.96 ± 0.2 | 38.77 ± 1.7 |
| PCL/AcEt8020 | 10.43 ± 1.2 | 1.36 ± 0.1 | 31.37 ± 2 |
| PCL/AcW9505 | 15.99 ± 0.7 | 0.81 ± 0.1 | 44.51± 0.9 |
| PCL/AcW9010 | 9.34 ± 3 | 1.45 ± 1.4 | 69.63 ± 3.7 |

To verify whether residual solvent or water could contribute to the observed mechanical behavior, thermogravimetric analysis was performed on both PLA and PCL membranes. The TGA curves show only negligible mass losses at low temperatures, indicating minimal residual content and exclude any significant plasticization effect (see Fig. S2).

In addition, differential scanning calorimetry (DSC) analysis revealed comparable degrees of crystallinity (Xc) for PCL and PLA-based membranes processed with both conventional and green solvent systems, indicating that the observed mechanical differences are primarily governed by morphological features rather than solvent-induced changes in polymer crystalline structure (see Fig. S3)

On the whole, the analysis confirmed that green solvents, particularly acetone/ethanol and acetone/water mixtures, exhibited mechanical performances fully comparable to those achieved with hazardous solvents such as chloroform and dichloromethane. In several cases, the properties were not only comparable but even improved, thus demonstrating the feasibility of replacing harmful solvents without compromising the mechanical performance of electrospun membranes.

Although the mechanical resistance is a primary requirement for membrane integrity, the performance of these materials is strongly influenced by their surface characteristics. For this reason, attention was then focused on evaluating the wettability of the membranes.

To evaluate the wettability of the membranes and gain further insight into their surface characteristics, wettability tests were performed using water and waste oil as liquids. This feature is crucial for many applications, especially for oil/water separation processes and for the selective absorption of contaminants. For this purpose, water contact angle (WCA) and oil contact angle (OCA) tests were performed to evaluate the hydrophobicity and oleophilicity of the membranes obtained from green solvents and to compare them with those prepared using the hazardous reference systems. The images of the contact angles and the values obtained from the tests, 1 s after the droplet touched the membrane surface, are shown in Figure 6.

The membranes obtained from the reference solvents systems, PLA/CHF and PCL/DCM, exhibited the typical hydrophobic and oleophilic character of these polymers, with WCA of 105° and 96°, respectively, and OCA close to 0°. The membranes produced using green solvent systems displayed comparable or slightly higher WCA values. In particular, PLA based membranes obtained by benign solvents systems showed WCA values between 108° and 129°, while PCL based membranes exhibited values ranging from 96° to 127°, confirming the overall hydrophobicity of both materials. Regarding oil wettability, all membranes showed very low OCA values (0–15°), indicative of pronounced oleophilicity and easy oil diffusion across the surface.

On the whole, these results confirm that the use of green solvents does not alter the hydrophobic and oleophilic behavior of PLA and PCL membranes.

The observed surface characteristics are consistent with previous reports on nanofibrous structures based on these polymers, which combine water repellency and oil affinity, making them promising candidates for oil/water separation and selective absorption applications [2,9,21].

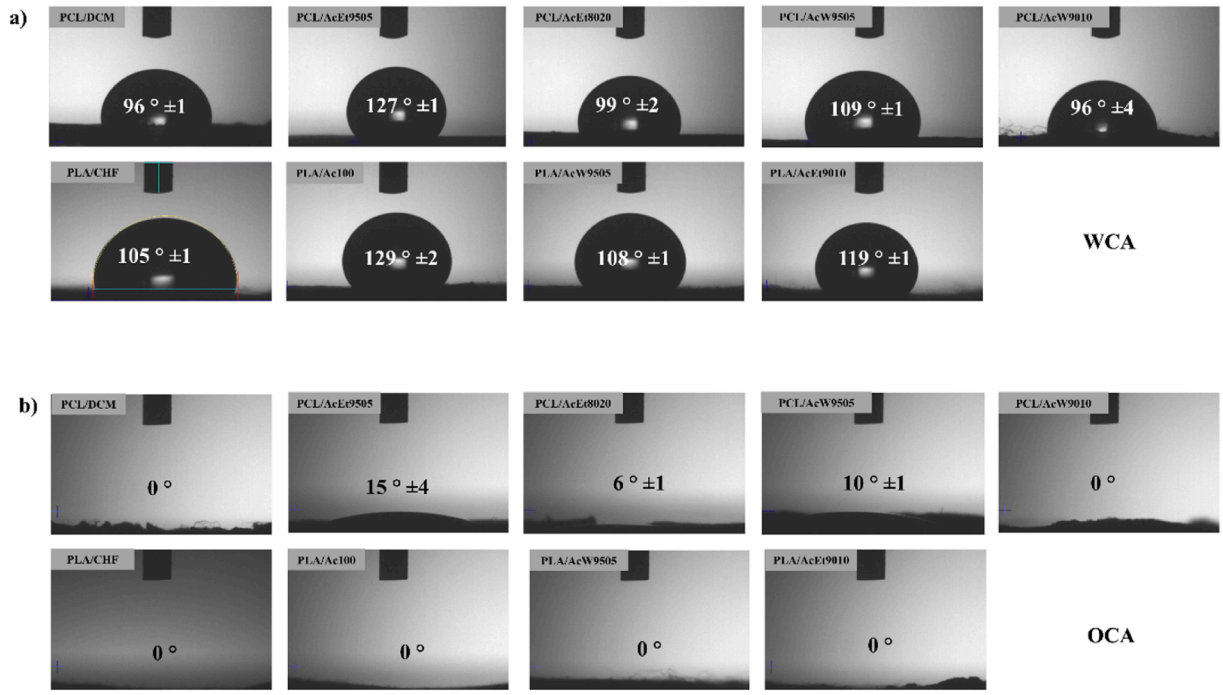


**Figure 6.** Water (WCA) and oil (OCA) contact angle measurements of PLA- and PCL-based membranes produced with hazardous and green solvent systems. All values were recorded 1 s after droplet deposition

The evidence of a hydrophobic and oleophilic surface, confirmed by wettability tests, suggests that the obtained membranes are particularly suitable for selective absorption processes. To verify this potential application, the absorption capacity of both vegetable and mineral oils was evaluated through oil spill clean-up tests conducted with olive oil and used motor oil (figure 7a-b).

The absorption tests in both used motor oil and olive oil (Figure 7a) show that all PLA membranes exhibit comparable performance, regardless of the solvent system. Specifically, for used motor oil, the absorption capacity ranges between 28 and 32 g/g, while for olive oil the values are slightly lower, between 20 and 24 g/g. No significant differences were observed among the hazardous reference (PLA/CHF) and PLA/Ac100 and PLA/AcEt9010. The only exception is the PLA/AcW9505 sample, which shows slightly higher absorption values in both oils. This improved performance can be attributed to its particular morphological features, in particular, the presence of thinner fibers and a more open and porous network increases the available surface area and facilitates capillary-driven oil uptake. Overall, the data indicate that the replacement of chloroform with acetone-, ethanol- or water-based systems does not compromise the absorption performance of PLA membranes.

The behaviour of PCL based (Figure 7b) membranes was more heterogeneous. The reference system PCL DCM showed intermediate absorption capacities (approximately 20-22 g/g for olive oil and similar values for used motor oil). Among the green systems, some differences were observed. In particular, PCL/AcEt9505 and PCL/AcEt8020 showed slightly lower values, while PCL/AcW9505 and PCL/AcW9010 achieved the highest performance, particularly with olive oil, reaching values above 25 g/g. In this case, the addition of water to the solvent system likely promoted the formation of thinner and more uniform fibers, increasing the available surface area for absorption. Figure 7a'-b' visually demonstrates, through a sequence of frame, the selective absorption of the membranes during oil spill clean-up tests with olive Fig.7a' and exhaust motor oils Fig.7b'.

In summary, the data confirm that green systems not only ensure absorption capacities comparable to those obtained with hazardous solvents but, in some cases (such as PCL with water-based systems), can even significantly improve performance, making the membranes particularly suitable for oil spill clean-up applications.

Figures 7c-d shows oil absorption behaviour as a function of time for PLA- and PCL-based membranes.

Regarding PLA-based membranes (Figure 7c), all the samples exhibit fast and overall homogeneous absorption kinetics. In particular, PLA/CHF reference sample achieves approximately 80 % of its final absorption capacity within the first 35-40 s, while the final plateau is achieved within about 55-60 s. A very similar behavior is observed for PLA/Ac100, which achieves about 80 % absorption within a comparable time interval (≈40 s) and shows a similar time to final saturation. PLA/AcEt9010 also displays comparable kinetics, reaching approximately 80 % of the absorbed weight within the first 40 s and achieving the final plateau within about 60 s. PLA/AcW9505 is characterized by a slightly faster absorption kinetics: in this case, approximately 80 % of the final absorption is achieved within the first 30 s, while the saturation plateau is established within about 45–50 s. This behaviour is consistent with the morphological features discussed above; in particular, the presence of thinner fibers and a more open fibrous network, which reasonably promote faster oil imbibition through capillary mechanisms.

The behavior of PCL-based membranes (Figure 7d) is more heterogeneous. Systems characterized by a predominantly fibrous and relatively uniform structure, namely PCL/DCM, PCL/AcEt8020, and PCL/AcW9505, exhibit rapid absorption kinetics, reaching approximately 80 % of the final absorption capacity within the first 35-40 s. In these cases, the saturation plateau is achieved in a time range of about 50-60 s.

In contrast, systems characterized by more heterogeneous and multimodal fibrous structures, such as PCL/AcEt9505 and PCL/

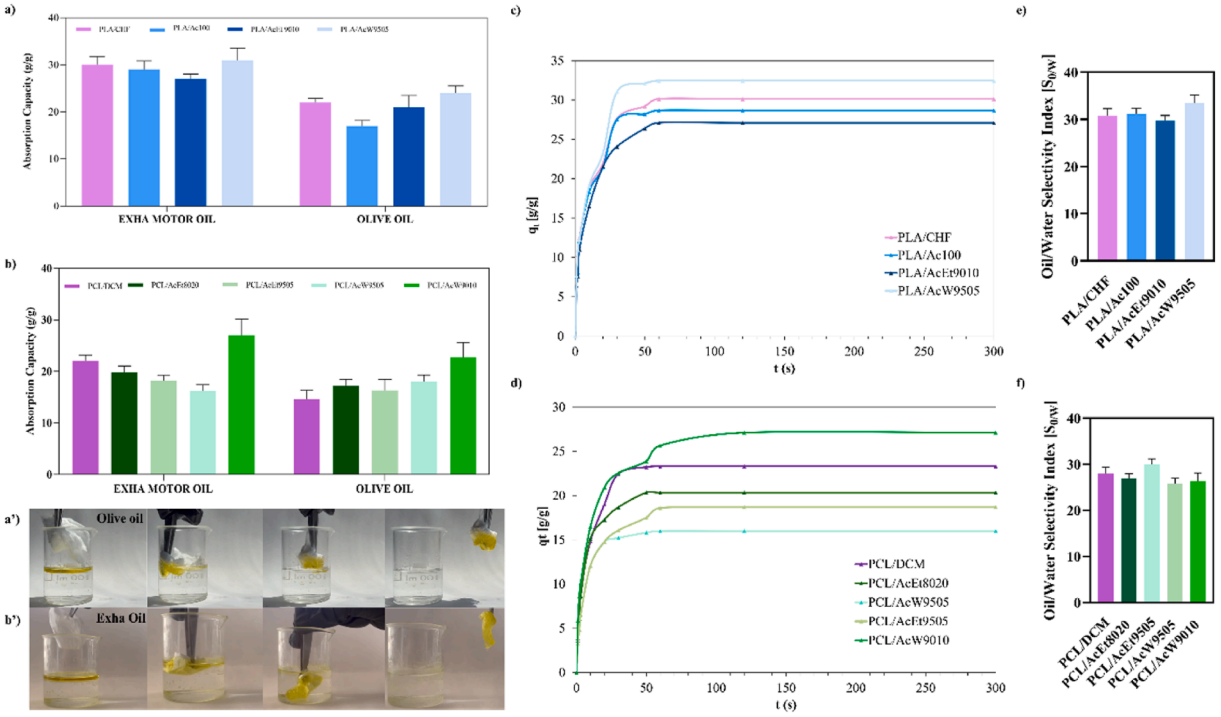


**Figure 7.** Absorption capacity of PLA a) and PCL b) membranes in exhaust motor oil and olive oil and photo that illustrate the oil spill removal test using the membranes, demonstrating their oleophilic behavior and practical applicability in oil-clean-up processes, oil spill clean-up photogram sequence of olive and exha motor oil a'), b') respectively, time-dependent oil absorption kinetics $q_{(t)}$ for PLA-based c) and PCL-based d) membranes, measured using exhaust motor oil, showing the evolution of absorbed oil as a function of time until saturation, oil-to-water selectivity index of PLA-based membranes, calculated as the ratio between oil and water absorption capacities e) and Oil-to-water selectivity index of PCL-based membranes f).

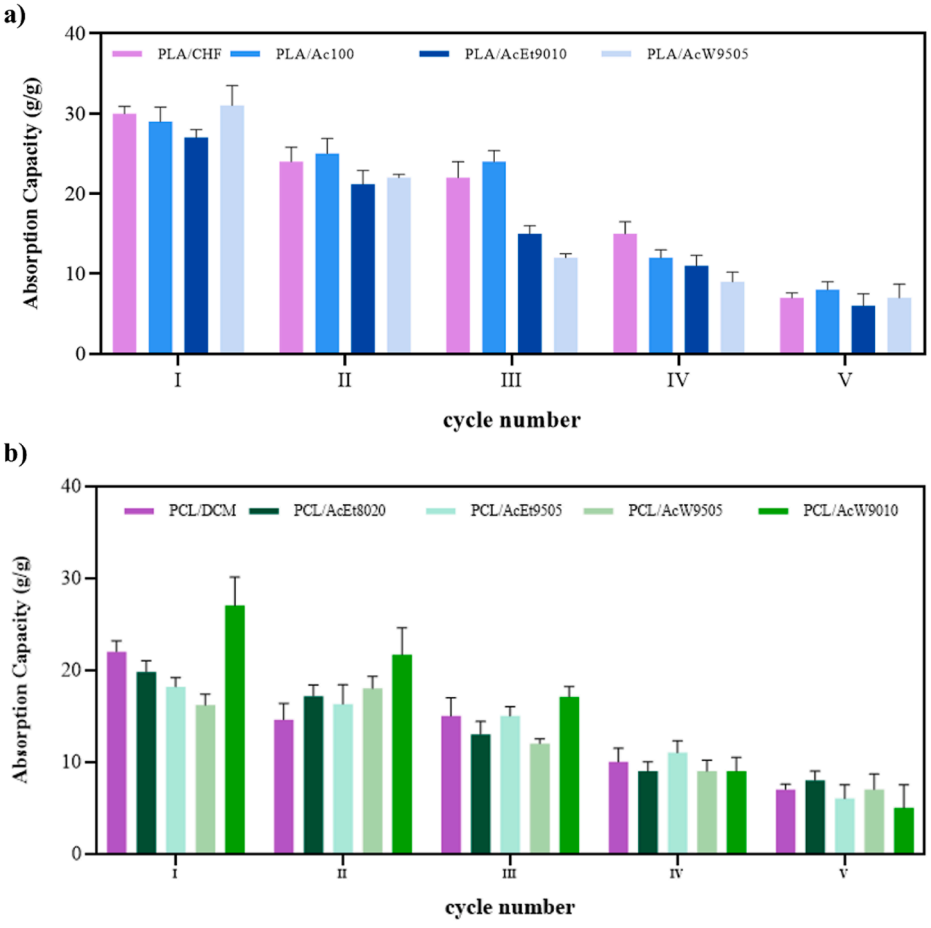


**Figure 8.** Reusability performance of PLA (a) and PCL (b) membranes over five oil absorption and recovery cycles using exhaust motor oil.

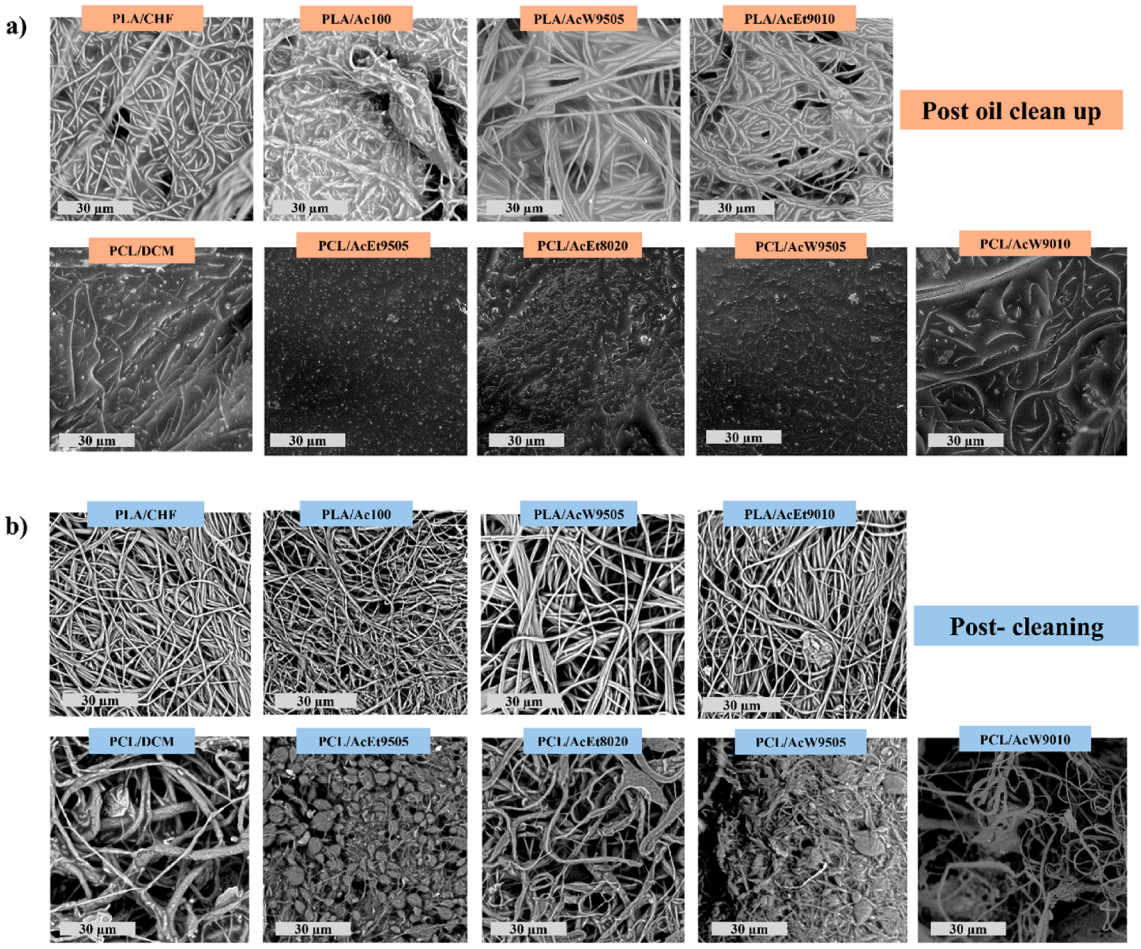


**Figure 9.** Morphological structure of PLA and PCL based membranes after (a) oil spill clean-up and (b) after the fifth absorption/desorption cycle.

**Table 6**
Comparison of the absorption capacity of PLA or PCL fibrous membranes produced using conventional and potentially carcinogenic solvent systems versus the green solvent systems proposed in this work.

| Based Materials | Process | Solvent System | Fillers | Absorption Capacity (g/g) | References |
|---|---|---|---|---|---|
| PLA 1 | Electrospinning | CHF/DMF | AKD | 15 | [74] |
| PLA 2 | Electrospinning | DCM | – | 27 | [75] |
| PLA 3 | Wet-electrospinning | CHF/Ac | PEO | 25 | [9] |
| PLA 4 | Electrospinning | TCM/DMSO | LDH AgGB | 20 | [76] |
| PCL 1 | Electrospinning | CHF | – | 12 | [77] |
| PCL 2 | Electrospinning | DCM/DMF | – | 30 | [78] |
| PCL 3 | Wet-electrospinning | DCM/Et | Graphene Oxide | 28 | [79] |
| ***PCL This work*** | ***Electrospinning*** | ***Ac/Et- Ac/W*** | ***-*** | ***25-28*** | ***This work*** |
| ***PLA This work*** | ***Electrospinning*** | ***Ac/Et- Ac/W*** | ***-*** | ***25-28*** | ***This work*** |

AcW9010, show slightly slower absorption kinetics. For both samples, approximately 80 % of the final absorption is achieved within the first 50 s. However, the final saturation plateau is observed at longer times, namely around 60 s for PCL/AcEt9505 and up to about 110 s for PCL/AcW9010. This behaviour can be likely attributed to the presence of less uniform structures and aggregates, which slow down the oil imbibition dynamics within the fibrous network.

The oil-to-water selectivity indices reported in Figures 7e and 7f further confirm the strong preferential affinity of all membranes toward oil with respect to water. All systems exhibit high selectivity values, indicating negligible water uptake compared to oil absorption, regardless of the polymer type or solvent system employed.

Overall, the selectivity indices remain consistently high across all samples, demonstrating that the adoption of green solvent systems does not compromise oil/water selectivity. In some cases, even slightly enhanced selectivity is observed, confirming that solvent substitution does not adversely affect the surface affinity of the membranes.

These results clearly demonstrate that the membranes behave as selective oil sorbents rather than non-selective sponge-like materials, fulfilling a key requirement for realistic oil spill clean-up applications [57, 72, 73].

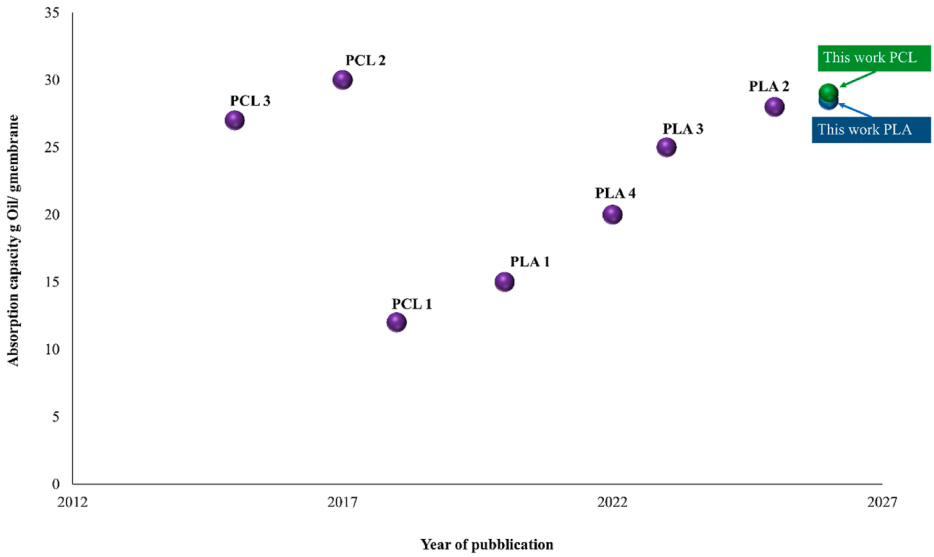


**Figure 10.** Absorption capacities of PLA and PCL-based membranes obtained in this work compared with reference literature studies, plotted against publication year.

To evaluate the reusability of the membranes, used motor oil was selected as the reference contaminant, since it represents a more complex material to capture and remove compared to vegetable oils. This choice allowed testing the performance of the materials under more realistic conditions, highlighting their actual robustness in application.

Figure 8 reports the evolution of the absorption capacity over five consecutive absorption-desorption cycles.

For both PLA systems (Fig 8a) and PCL systems (figure 8b). The results show that, for all the systems analyzed, the absorption capacity remained almost stable during the first cycles, with a progressive reduction starting from the third/fourth cycle. Consistently with what has been reported in the literature [9], a more pronounced decline was observed around the fifth cycle, indicating progressive fiber saturation and partial loss of the original structure.

This behaviour indicate that membranes produced with benign solvents are not only comparable to those obtained with hazardous solvents at their first use but also exhibit good structural resistance upon reuse, confirming their suitability for environmental remediation.

After evaluating the absorption performance over multiple cycles, it was necessary to verify whether the repeated use affected the structural integrity of the membranes.

Figure 9 shows the SEM micrographs of PLA and PCL based membranes after the first oil spill clean-up test (Fig. 9a) and following the fifth absorption–desorption cycle (Fig. 9b). The images reveal that the fibrous structures maintained their morphology, with no significant changes in fiber diameter, shape, or surface texture, and no evidence of breakage or fusion. The observed morphological across all samples indicates a high resistance to degradation and confirms the robustness and reproducibility of the fabrication process. These results demonstrate that the membranes preserve their performance relevant architecture even after multiple use and washing cycles, supporting their suitability for repeated environmental remediation processes.

Since the systems maintained good structural stability and satisfactory performance in terms of both mechanics and functionality, it is worth comparing the results obtained with other systems already reported in the literature.

Table 6 reports the main processing parameters and oil absorption capacities of electrospun PLA and PCL based membranes from previous studies, whereas Figure 10 shows the comparison with the membranes developed in this work.

Although many of the reported systems were produced using hazardous and non-sustainable solvents such as chloroform, dichloromethane, or trichloromethane, and were often enhanced with nanofillers or hydrophobic additives to improve oil affinity, their absorption capacities generally range between 15 and 30 g/g.

In contrast, the green-solvent-based membranes developed in this study achieved an absorption capacity of 25-28 g/g for both PLA and PCL, demonstrating that sustainable fabrication routes can deliver comparable or even superior performance without relying on hazardous solvents or additional chemical modifications.

Beyond performance aspects, it is also useful to reflect on sustainability. Without entering into the details of a full LCA, data available in the literature indicate that chlorinated solvents such as chloroform present a significantly higher cumulative energy demand (CED), exceeding 100 MJ/kg, together with a well-documented environmental and health impact, and are classified as potentially carcinogenic under European regulations.

In contrast, acetone, used here as a green acceptable alternative, has a lower CED (approximately 60–70 MJ/kg), is readily biodegradable, and is not classified as carcinogenic. This simple qualitative comparison highlights how the replacement of conventional solvents with green alternatives can lead not only to a reduction of health risks but also to a concrete decrease in the energy and environmental footprint of the process.

Finally, safety aspects should be emphasized. In particular, the use of chlorinated solvents such as chloroform and dichloromethane requires strict containment measures in both laboratory and industrial settings (fume hoods, personal protective equipment, dedicated disposal procedures), which entail high costs and significant risks for operators. The adoption of solvents such as acetone, ethanol, and water substantially reduces these constraints, allowing safer and more sustainable process management and enhancing the acceptability of the method in both academic and industrial contexts.

## 4. Conclusions

This study was motivated by the aim of assessing the possibility of replacing hazardous solvents traditionally employed for the

electrospinning of widely used polymers such as PLA and PCL with more sustainable alternatives, thereby laying the groundwork for overcoming the techno-scientific lock-in of the solution electrospinning process.

The preliminary analysis of thermodynamic compatibility, followed by the experimental evaluation of the solutions, enabled the identification of green solvent systems capable of ensuring stability and processability during electrospinning, without the need to modify the process parameters commonly adopted in both scientific and industrial contexts.

In this context, the proposed approach inherently addresses several of the principles of green membrane materials and processes, particularly those related to the use of benign solvents, process safety, energy efficiency, and compatibility with scalable manufacturing routes [41].

The resulting membranes exhibited morphological, mechanical, and functional properties fully comparable, and in some cases even superior, to those prepared with the hazardous reference solvents, thus confirming the feasibility of replacing CHF and DCM without significant compromises in performance.

Overall, the results clearly demonstrate that it is realistic to begin considering the overcoming of the techno-scientific lock-in in polymer electrospinning, with evident benefits in terms of reduced production costs, lower environmental impact, and, most importantly, enhanced safety for both operators and end users.

## CRediT authorship contribution statement

**Emmanuel Fortunato Gulino:** Writing – review & editing, Writing – original draft, Visualization, Validation, Software, Methodology, Investigation, Formal analysis, Data curation, Conceptualization. **Roberto Scaffaro:** Writing – review & editing, Validation, Supervision, Resources, Project administration, Funding acquisition.

## Funding

The author(s) disclosed receipt of the following financial support for the research, authorship, and/or publication of this article: This work was supported by the SAMOTHRACE (Sicilian micro and nano technology research and innovation center) Extended Partnership and received funding from the European Union Next-GenerationEU (PIANO NAZIONALE DI RIPRESA E RESILIENZA (PNRR) – MISSIONE 4 COMPONENTE 2, INVESTIMENTO 1.5) European Commission (ECS_00000022)

## Declaration of interests

The authors declare that they have no known competing financial interest or personal relationships that could have appeared to influence the work reported in this paper.

## Appendix A. Supplementary data

Supplementary data to this article can be found online at https://doi.org/10.1016/j.aiepr.2026.02.001.

## References

[1] Y. Cho, J.W. Beak, M. Sagong, S. Ahn, J.S. Nam, I.D. Kim, Electrospinning and nanofiber technology: fundamentals, innovations, and applications, Adv. Mater. 37 (2025) 2500162, https://doi.org/10.1002/ADMA.202500162;REQUESTEDJOURNAL:JOURNAL:15214095;WGROUP:STRING:PUBLICATION.

[2] R. Sarbatly, D. Krishnaiah, Z. Kamin, A review of polymer nanofibres by electrospinning and their application in oil–water separation for cleaning up marine oil spills, Mar. Pollut. Bull. 106 (2016) 8–16, https://doi.org/10.1016/J.MARPOLBUL.2016.03.037.

[3] C. Wang, W. Wang, H. Qi, Y. Dai, S. Jiang, B. Ding, et al., Electrospinning and electrospun nanofibers: from academic research to industrial production, Prog Mater Sci 154 (2025) 101494, https://doi.org/10.1016/J.PMATSCI.2025.101494.

[4] G.F. Elfawal, A.O. Šišková, A.E. Andicsová, Gomaa, F. Elfawal, A. Eckstein, et al., Electrospinning: a game-changer in fiber production and practical applications, Fibers and Polymers 26 (10) (2025) 4133–4160, https://doi.org/10.1007/S12221-025-01105-W, 2025;26.

[5] M.K. Gaydhane, C.S. Sharma, S. Majumdar, Electrospun nanofibres in drug delivery: advances in controlled release strategies, RSC Adv 13 (2023) 7312–7328, https://doi.org/10.1039/D2RA06023J.

[6] S. Thakkar, M. Misra, Electrospun polymeric nanofibers: new horizons in drug delivery, Eur. J. Pharmaceut. Sci. 107 (2017) 148–167, https://doi.org/10.1016/J.EJPS.2017.07.001.

[7] E.F. Gulino, M.C. Citarrella, A. Maio, R. Scaffaro, An innovative route to prepare in situ graded crosslinked PVA graphene electrospun mats for drug release, Compos Part A Appl Sci Manuf 155 (2022) 106827, https://doi.org/10.1016/J.COMPOSITESA.2022.106827.

[8] R. Scaffaro, L. Settanni, E.F. Gulino, Release profiles of carvacrol or chlorhexidine of PLA/Graphene nanoplatelets membranes prepared using electrospinning and solution blow spinning: a comparative Study, Molecules 28 (2023), https://doi.org/10.3390/MOLECULES28041967. Page 1967 2023;28:1967.

[9] R. Scaffaro, E.F. Gulino, M.C. Citarrella, Biodegradable membrane with high porosity and hollow structure obtained via electrospinning for oil spill Clean-up application, J Polym Environ 31 (2023) 3965–3981, https://doi.org/10.1007/s10924-023-02876-0.

[10] R. Scaffaro, M. Gammino, A. Maio, Wet electrospinning-aided self-assembly of multifunctional GO-CNT@PCL core-shell nanocomposites with spider leg bioinspired hierarchical architectures, Compos. Sci. Technol. 221 (2022) 109363, https://doi.org/10.1016/J.COMPSCITECH.2022.109363.

[11] R. Scaffaro, A. Maio, M. Gammino, Electrospun polymeric nanohybrids with outstanding pollutants adsorption and electroactivity for water treatment and sensing devices, Adv Compos Hybrid Mater 7 (2024) 1–19, https://doi.org/10.1007/S42114-023-00827-W/FIGURES/12.

[12] M. Milazzo, S. Danti, P. Livens, J. Dirckx, R. Scaffaro, M. Gammino, Electrospun graphene oxide/polymeric nanocomposites for eardrum replacements, Compos. Commun. 51 (2024) 102048, https://doi.org/10.1016/J.COCO.2024.102048.

[13] H. Yu, J. Zhao, Y. Zhang, M. Zhang, X. Sun, X. Hao, et al., Associations between long-term exposure to particulate matter and mortality from multiple causes among the oldest-old people, J Hazard Mater 494 (2025) 138434, https://doi.org/10.1016/J.JHAZMAT.2025.138434.

[14] R. Shen, Z. Shao, J. Xie, H. Li, Z. Zeng, J. Jiang, et al., Biobased nanofibrous membrane via delayed-volatilizing green electrospinning for high-performance air filtration, ACS Appl. Polym. Mater. 5 (2023) 8559–8569, https://doi.org/10.1021/ACSAPM.3C01666.

[15] G. Zheng, Z. Gui, Q. Wang, R. Chen, R. Shen, S. Guo, et al., Green electrospinning fully bio-based lightweight nanofibrous membrane for high-performance and antibacterial air filtration via small molecule mutual support mechanism, J Clean Prod 486 (2025) 144562, https://doi.org/10.1016/J.JCLEPRO.2024.144562.

[16] Z. Shao, Q. Wang, Z. Gui, R. Shen, R. Chen, Y. Liu, et al., Electrospun bimodal nanofibrous membranes for high-performance, multifunctional, and lightweight air filtration: a review, Sep. Purif. Technol. 358 (2025) 130417, https://doi.org/10.1016/J.SEPPUR.2024.130417.

[17] R. Scaffaro, E. Gulino, F. Lopresti, Structure-Property Relationship and Controlled Drug Release from Multiphasic Electrospun carvacrol-embedded Polylactic acid/polyethylene Glycol and Polylactic acid/ Polyethylene Oxide Nanofiber Mats, 49, 2020, pp. 943–966, https://doi.org/10.1177/1528083718801359.

[18] R. Scaffaro, A. Maio, E.F. Gulino, G.D.M. Micale, PLA-based functionally graded laminates for tunable controlled release of carvacrol obtained by combining electrospinning with solvent casting, React Funct Polym 148 (2020), https://doi.org/10.1016/j.reactfunctpolym.2020.104490.

[19] E. Malikmammadov, T.E. Tanir, A. Kiziltay, V. Hasirci, N. Hasirci, PCL and PCL-based Materials in Biomedical Applications, 29, 2017, pp. 863–893, https://doi.org/10.1080/09205063.2017.1394711.

[20] F. Hadizadeh, E. Khodaverdi, F. Oroojalian, P. Rahmanian-Devin, S. Hassan, N. Omidkhah, et al., Preparation of porous PCL-PEG-PCL scaffolds using supercritical carbon dioxide, Int J Pharm 631 (2023) 122507, https://doi.org/10.1016/J.IJPHARM.2022.122507.

[21] R. Scaffaro, F. Lopresti, V. Catania, S. Santisi, S. Cappello, L. Botta, et al., Polycaprolactone-based scaffold for oil-selective sorption and improvement of bacteria activity for bioremediation of polluted water: porous PCL system obtained by leaching melt mixed PCL/PEG/NaCl composites: oil uptake performance and bioremediation efficiency, Eur. Polym. J. 91 (2017) 260–273, https://doi.org/10.1016/J.EURPOLYMJ.2017.04.015.

[22] G. Malaguarnera, E. Cataudella, M. Giordano, G. Nunnari, G. Chisari, M. Malaguarnera, Toxic hepatitis in occupational exposure to solvents, World Journal of Gastroenterology : WJG 18 (2012) 2756, https://doi.org/10.3748/WJG.V18.I22.2756.

[23] C. McDermott, J.J.A. Heffron, Toxicity of industrially relevant chlorinated organic solvents In vitro, Int J Toxicol 32 (2013) 136–145, https://doi.org/10.1177/1091581813482006.
[24] R.H. McKee, M.D. Adenuga, J.C. Carrillo, Characterization of the toxicological hazards of hydrocarbon solvents, Crit Rev Toxicol 45 (2015) 273–365, https://doi.org/10.3109/10408444.2015.1016216. PAGE:STRING:ARTICLE/CHAPTER.
[25] Electrospinning Based on Benign Solvents: Current Definitions, Implications and Strategies - Green Chemistry (RSC Publishing) DOI:10.1039/D1GC04252A n.d. https://pubs.rsc.org/en/content/articlehtml/2022/gc/d1gc04252a (accessed October 31, 2025).
[26] A.R. D'Amato, M.T.K. Bramson, D.T. Corr, D.L. Puhl, R.J. Gilbert, J. Johnson, Solvent retention in electrospun fibers affects scaffold mechanical properties, Electrospinning 2 (2018) 15, https://doi.org/10.1515/ESP-2018-0002.
[27] A.A. Conte, X. Hu, V. Beachley, Role of draw rate and molecular weight when Electrospun nanofibers are post-drawn with residual solvent, Macromol Mater Eng 308 (2023) 2200475, https://doi.org/10.1002/MAME.202200475;WGROUP:STRING:PUBLICATION.
[28] J. Nam, Y. Huang, S. Agarwal, J. Lannutti, Materials selection and residual solvent retention in biodegradable electrospun fibers, J Appl Polym Sci 107 (2008) 1547–1554, https://doi.org/10.1002/APP.27063;REQUESTEDJOURNAL:JOURNAL:10974628. PAGE:STRING:ARTICLE/CHAPTER.
[29] A.R. D'Amato, N.J. Schaub, J.M. Cardenas, E. Franz, D. Rende, A.M. Ziemba, et al., Evaluation of procedures to quantify solvent retention in electrospun fibers and facilitate solvent removal, Fibers and Polymers 18 (3) (2017) 483–492, https://doi.org/10.1007/S12221-017-1061-5, 2017;18.
[30] A.R. D'Amato, N.J. Schaub, J.M. Cardenas, A.S. Fiumara, P.M. Troiano, A. Fischetti, et al., Removal of retained electrospinning solvent prolongs drug release from electrospun PLLA fibers, Polymer (Guildf.) 123 (2017) 121–127, https://doi.org/10.1016/J.POLYMER.2017.07.008.
[31] C. Capello, U. Fischer, K. Hungerbühler, What is a green solvent? A comprehensive framework for the environmental assessment of solvents, Green Chem. 9 (2007) 927–934, https://doi.org/10.1039/B617536H.
[32] J.M. Anaya-Mancipe, A.C. de Figueiredo, L.G. Rabello, M.L. Dias, R.M. da Silva Moreira Thiré, Evaluation of the polycaprolactone hydrolytic degradation in acid solvent and its influence on the electrospinning process, J Appl Polym Sci 141 (2024) e55662, https://doi.org/10.1002/APP.55662;CTYPE:STRING:JOURNAL.
[33] M. Borrotti, E. Lanzarone, F. Manganini, S. Ortelli, A. Pievatolo, C. Tonetti, Defect minimization and feature control in electrospinning through design of experiments, J Appl Polym Sci 134 (2017) 44740, https://doi.org/10.1002/APP.44740. REQUESTEDJOURNAL:JOURNAL:10974628;PAGE:STRING:ARTICLE/CHAPTER.
[34] Z. Li, C. Zhu, X. He, Z. Teng, W. Liu, Y. Zhang, et al., One stone kills two birds: novel recycled fiber spinning engineering for one-step yarn reinforcement and clean dyeing, Fundam. Res. (2025), https://doi.org/10.1016/J.FMRE.2025.02.018.
[35] L. Lovecká, M. Kovářová, D. Hanušová, D. Kimmer, A. Poláchová, V. Sedlařík, Application of green solvents as a replacement of toxic dimethylformamide in the polylactic acid electrospinning process, Sustain. Mater. Technol. 44 (2025) e01405, https://doi.org/10.1016/J.SUSMAT.2025.E01405.
[36] C. Yang, F. Topuz, S.H. Park, G. Szekely, Biobased thin-film composite membranes comprising priamine–genipin selective layer on nanofibrous biodegradable polylactic acid support for oil and solvent-resistant nanofiltration, Green Chem. 24 (2022) 5291–5303, https://doi.org/10.1039/D2GC01476A.
[37] Y. Tian, Y. Chen, S. Wang, X. Wang, J. Yu, S. Zhang, et al., Ultrathin aerogel-structured micro/nanofiber metafabric via dual air-gelation synthesis for self-sustainable heating, Nat. Commun. 15 (1) (2024) 6416, https://doi.org/10.1038/s41467-024-50654-w, 2024;15.
[38] A. Chiloeches, R. Cuervo-Rodríguez, Y. Gil-Romero, M. Fernández-García, C. Echeverría, A. Muñ Oz-Bonilla, Electrospun Polylactic Acid-Based Fibers Loaded with Multifunctional Antibacterial Biobased Polymers, 2022, https://doi.org/10.1021/acsapm.2c00928.
[39] J. Ge, X. Lv, J. Zhou, Y. Lv, J. Sun, H. Guo, et al., Multi-level structured polylactic acid electrospun fiber membrane based on green solvents for high-performance air filtration, Sep. Purif. Technol. 331 (2024) 125659, https://doi.org/10.1016/J.SEPPUR.2023.125659.
[40] D.G. Oldal, F. Topuz, T. Holtzl, G. Szekely, Green electrospinning of biodegradable cellulose acetate nanofibrous membranes with tunable porosity, ACS Sustain Chem Eng 11 (2023) 994–1005, https://doi.org/10.1021/ACSSUSCHEMENG.2C05676.
[41] The 12 Principles of Green Membrane Materials and Processes for Realizing the United Nations' Sustainable Development Goals - RSC Sustainability (RSC Publishing) DOI:10.1039/D4SU00027G n.d. https://pubs.rsc.org/en/content/articlehtml/2024/su/d4su00027g (accessed January 26, 2026).
[42] A. Keirouz, F. Galiano, F. Russo, E. Fontananova, B. Castro-Dominguez, A. Figoli, et al., Cyrene-Enabled green electrospinning of nanofibrous graphene-based membranes for water desalination via membrane distillation, ACS Sustain Chem Eng 12 (2024) 17713–17725, https://doi.org/10.1021/ACSSUSCHEMENG.4C06363.
[43] R. Chen, Q. Wang, R. Shen, Z. Gui, Y. Yan, M. Tang, et al., Green and efficient electrospinning of ethyl cellulose-based nanofibrous membrane for high-performance and antibacterial air filtration, Carbohydr Polym 366 (2025) 123893, https://doi.org/10.1016/J.CARBPOL.2025.123893.
[44] P. Bhattacharjee, D. Naskar, H.W. Kim, T.K. Maiti, D. Bhattacharya, S.C. Kundu, Non-mulberry silk fibroin grafted PCL nanofibrous scaffold: promising ECM for bone tissue engineering, Eur. Polym. J. 71 (2015) 490–509, https://doi.org/10.1016/J.EURPOLYMJ.2015.08.025.
[45] R. Bakhshi, M. Mohammadi-Zerankeshi, M. Mehrabi-Dehdezi, R. Alizadeh, S. Labbaf, P. Abachi, Additive manufacturing of PLA-Mg composite scaffolds for hard tissue engineering applications, J Mech Behav Biomed Mater 138 (2023) 105655, https://doi.org/10.1016/J.JMBBM.2023.105655.
[46] R. Ghafari, R. Scaffaro, A. Maio, E.F. Gulino, G. Lo Re, M. Jonoobi, Processing-structure-property relationships of electrospun PLA-PEO membranes reinforced with enzymatic cellulose nanofibers, Polym. Test. 81 (2020), https://doi.org/10.1016/j.polymertesting.2019.106182.
[47] R. Scaffaro, A. Maio, E.F. Gulino, G.D.M. Micale, PLA-based functionally graded laminates for tunable controlled release of carvacrol obtained by combining electrospinning with solvent casting, React Funct Polym 148 (2020) 104490, https://doi.org/10.1016/J.REACTFUNCTPOLYM.2020.104490.
[48] A. Malara, Environmental concerns on the use of the electrospinning technique for the production of polymeric micro/nanofibers, Sci. Rep. 14 (1) (2024) 1–11, https://doi.org/10.1038/s41598-024-58936-5, 2024;14.
[49] K. Moradi, M.D. Firouzjaei, M. Elliott, M. Sadrzadeh, Lifecycle assessment of membrane synthesis for the application of thermo-osmotic energy conversion process, Case Stud. Chem. Environ. Eng. 10 (2024) 100847, https://doi.org/10.1016/J.CSCEE.2024.100847.
[50] C. Bordes, V. Fréville, E. Ruffin, P. Marote, J.Y. Gauvrit, S. Briançon, et al., Determination of poly(ε-caprolactone) solubility parameters: application to solvent substitution in a microencapsulation process, Int J Pharm 383 (2010) 236–243, https://doi.org/10.1016/J.IJPHARM.2009.09.023.
[51] K.G. Patel, R.K. Maynard, L.S. Ferguson, M.L. Broich, J.C. Bledsoe, C.C. Wood, et al., Experimentally determined Hansen solubility parameters of biobased and biodegradable polyesters, ACS Sustain Chem Eng 12 (2024) 2386–2393, https://doi.org/10.1021/ACSSUSCHEMENG.3C07284.
[52] C.M. Hansen, Methods of characterization - surfaces, in: Hansen Solubility Parameters: a Users Handbook, Second Edition, 2007, pp. 113–123, https://doi.org/10.1201/9781420006834/HANSEN-SOLUBILITY-PARAMETERS-CHARLES-HANSEN/RIGHTS-AND-PERMISSIONS.
[53] R. Scaffaro, A. Maio, E.F. Gulino, B. Megna, Structure-property relationship of PLA-Opuntia Ficus Indica biocomposites, Compos. B Eng. 167 (2019) 199–206, https://doi.org/10.1016/J.COMPOSITESB.2018.12.025.
[54] O.F. Solomon, I.Z. Ciută, Détermination de la viscosité intrinsèque de solutions de polymères par une simple détermination de la viscosité, J Appl Polym Sci 6 (1962) 683–686, https://doi.org/10.1002/APP.1962.070062414. REQUESTEDJOURNAL:JOURNAL:10974628;PAGE:STRING:ARTICLE/CHAPTER.
[55] B.L. Hager, G.C. Berry, MODERATELY CONCENTRATED SOLUTIONS OF POLYSTYRENE - 1. VISCOSITY AS A FUNCTION OF CONCENTRATION, TEMPERATURE, AND MOLECULAR WEIGHT, Journal of Polymer Science Part A-2, Polymer Physics 20 (1982) 911–928, https://doi.org/10.1002/POL.1982.180200513. SUBPAGE:STRING:ABSTRACT;WEBSITE:WEBSITE:PERICLES;ISSUE:ISSUE:DOI.
[56] M. Erencia, F. Cano, J.A. Tornero, J. Macanás, F. Carrillo, Resolving the electrospinnability zones and diameter prediction for the electrospinning of the Gelatin/Water/Acetic Acid System, Langmuir 30 (2014) 7198–7205, https://doi.org/10.1021/LA501183F.
[57] H.M. Yesuf, M.H. Aweke, S.R. Islam, X. Zhang, X. Qin, Multi-Fiber blended needle-punched nonwoven With oleophilic and self-cleaning properties for oil spill cleanup, Adv Mater Technol 10 (2025) 2401628, https://doi.org/10.1002/ADMT.202401628;WGROUP:STRING:PUBLICATION.
[58] A. Maio, M. Gammino, E.F. Gulino, B. Megna, P. Fara, R. Scaffaro, Rapid one-step fabrication of graphene oxide-decorated polycaprolactone three-dimensional templates for water treatment, ACS Appl. Polym. Mater. 2 (2020) 4993–5005, https://doi.org/10.1021/ACSAPM.0C00852/SUPPL_FILE/AP0C00852_SI_002.MPG.
[59] A. Subbotin, V. Kulichikhin, Orientation and aggregation of polymer chains in the straight electrospinning jet, Materials 13 (2020) 4295, https://doi.org/10.3390/MA13194295, 2020;13:4295.
[60] S.L. Shenoy, W.D. Bates, H.L. Frisch, G.E. Wnek, Role of chain entanglements on fiber formation during electrospinning of polymer solutions: good solvent, non-specific polymer–polymer interaction limit, Polymer (Guildf.) 46 (2005) 3372–3384, https://doi.org/10.1016/J.POLYMER.2005.03.011.
[61] A. Maio, M. Gammino, E.F. Gulino, B. Megna, P. Fara, R. Scaffaro, Rapid one-step fabrication of graphene oxide-decorated polycaprolactone three-dimensional templates for water treatment, ACS Appl. Polym. Mater. 2 (2020) 4993–5005, https://doi.org/10.1021/ACSAPM.0C00852/ASSET/IMAGES/LARGE/AP0C00852_0010.JPEG.
[62] R. Scaffaro, M.C. Citarrella, Stable and reusable electrospun bio-composite fibrous membranes based on PLA and natural fillers for air filtration applications, Sustain. Mater. Technol. 42 (2024) e01146, https://doi.org/10.1016/J.SUSMAT.2024.E01146.
[63] J. Ge, D. Han, S. Li, J. Li, S. Hong, C. Wang, et al., Electrospun membrane of PLA/calendula with improved UV protection and stable filtration performance, Sep. Purif. Technol. 344 (2024) 127310, https://doi.org/10.1016/J.SEPPUR.2024.127310.
[64] N. Dalton, R.P. Lynch, M.N. Collins, M. Culebras, Thermoelectric properties of electrospun carbon nanofibres derived from lignin, Int J Biol Macromol 121 (2019) 472–479, https://doi.org/10.1016/J.IJBIOMAC.2018.10.051.
[65] S. Basu, N. Gogoi, S. Sharma, M. Jassal, A.K. Agrawal, Role of elasticity in control of diameter of electrospun PAN nanofibers, Fibers and Polymers 14 (2013) 950–956, https://doi.org/10.1007/s12221-013-0950-5.

[66] A.A. Ali, M.A. El-Hamid, Electro-spinning optimization for precursor carbon nanofibers, Compos Part A Appl Sci Manuf 37 (2006) 1681–1687, https://doi.org/10.1016/J.COMPOSITESA.2005.10.008.
[67] R. Yaseri, M. Fadaie, E. Mirzaei, H. Samadian, A. Ebrahiminezhad, Surface modification of polycaprolactone nanofibers through hydrolysis and aminolysis: a comparative study on structural characteristics, mechanical properties, and cellular performance, Sci. Rep. 13 (1) (2023) 9434, https://doi.org/10.1038/s41598-023-36563-w, 2023;13.
[68] G.H. Kim, Electrospun PCL Nanofibers with Anisotropic Mechanical Properties as a Biomedical Scaffold, 2008, https://doi.org/10.1088/1748-6041/3/2/025010.
[69] F. Croisier, A.S. Duwez, C. Jérôme, A.F. Léonard, K.O. Van Der Werf, P.J. Dijkstra, et al., Mechanical testing of electrospun PCL fibers, Acta Biomater. 8 (2012) 218–224, https://doi.org/10.1016/J.ACTBIO.2011.08.015.
[70] N. Alharbi, M. Guthold, Mechanical properties of hydrated electrospun polycaprolactone (PCL) nanofibers, J Mech Behav Biomed Mater 155 (2024) 106564, https://doi.org/10.1016/J.JMBBM.2024.106564.
[71] D. Kai, M.P. Prabhakaran, G. Jin, S. Ramakrishna, Guided orientation of cardiomyocytes on electrospun aligned nanofibers for cardiac tissue engineering, J Biomed Mater Res B Appl Biomater 98 B (2011) 379–386, https://doi.org/10.1002/JBM.B.31862;JOURNAL:JOURNAL:15524981;WGROUP:STRING:PUBLICATION.
[72] P. Azmoon, M. Farhadian, A. Pendashteh, A.H. Navarchian, Fabrication of porous and conductive polystyrene/polyaniline fibers via electrospinning method: adsorption and selectivity of oil, Journal of Polymer Research 32 (3) (2025) 88, https://doi.org/10.1007/S10965-025-04299-Y, 2025;32.
[73] W. Guo, J. Yuan, X. Gao, Z. Wang, Y. Chen, L. Zhao, et al., Design of cell structures in PLA-based foams via supercritical $CO_2$ foaming: enabling ultrafast and high-capacity oil adsorption, Sep. Purif. Technol. 382 (2026) 135870, https://doi.org/10.1016/J.SEPPUR.2025.135870.
[74] C. Eang, P. Opaprakasit, Electrospun nanofibers with superhydrophobicity derived from degradable polylactide for Oil/Water separation applications, Journal of Polymers and the Environment 28 (5) (2020) 1484–1491, https://doi.org/10.1007/S10924-020-01704-Z, 2020;28.
[75] X. Li, K. Teng, J. Shi, W. Wang, Z. Xu, H. Deng, et al., Electrospun preparation of polylactic acid nanoporous fiber membranes via thermal-nonsolvent induced phase separation, J Taiwan Inst Chem Eng 60 (2016) 636–642, https://doi.org/10.1016/J.JTICE.2015.11.012.
[76] X.Q. Cheng, W. Liu, C. Zhang, X.C. Chen, S.Q. Duan, H. Fu, Synthesis and electrospinning of multiscale-ordered PLA/LDH@AgGB composite nanofibrous membrane for antibacterial and oil–water separation, J Appl Polym Sci 139 (2022) e52621, https://doi.org/10.1002/APP.52621;WGROUP:STRING:PUBLICATION.
[77] Enhanced Oil Removal from Water in Oil Stable Emulsions Using Electrospun Nanocomposite Fiber Mats - RSC Advances (RSC Publishing) DOI:10.1039/C7RA12646H n.d. https://pubs.rsc.org/en/content/articlehtml/2017/sc/c7ra12646h (accessed October 31, 2025).
[78] C.R. Reshmi, S.P. Sundaran, A. Juraij, S. Athiyanathil, Fabrication of superhydrophobic polycaprolactone/beeswax electrospun membranes for high-efficiency oil/water separation, RSC Adv 7 (2017) 2092–2102, https://doi.org/10.1039/C6RA26123J.
[79] R. Scaffaro, M. Gammino, 3D wet-electrospun “branch leaf” graphene oxide polycaprolactone fibers structure for enhancing oil-water separation treatment performance in a multi-scale design, Sustain. Mater. Technol. 43 (2025) e01200, https://doi.org/10.1016/J.SUSMAT.2024.E01200.